CATRINA (2024), 31(1):1-23

Monitoring Coastline Dynamics Using Satellite Remote Sensing and Geographic Information Systems: A Review of Global Trends

Kamal Srogy Darwish
Department of Geography, Faculty of Arts, Minia University, El Minia, 61519, Egypt

Received: September 24, 2023; accepted: April 24, 2024

ABSTRACT

Nearly half of the world's population lives near the coasts of oceans and seas. The coastline position changes under the influence of multiple natural and anthropogenic factors. Recently, due to the global impacts of climate change and population growth, the issue of geomorphological changes in coastlines has become more critical. Therefore, the assessment and mapping of coastline dynamics is one of the most essential factors for sustainable development goals and urban planning. The objectives of this study are to focus on discussing the research progress of applications of satellite remote sensing datasets and GIS methods for coastline extraction, mapping, and analysis along global coasts. A systematic review and trend analysis of the most recent published studies that focused on remote sensing and GIS techniques for assessing coastal dynamics were published between 2012 and 2022 along different coasts worldwide. The results indicated that multisource and multisensor remote sensing datasets were globally utilized for monitoring coastline changes, including (1) medium-resolution imagery such as Sentinel and Landsat, (2) SAR and optical high-resolution imagery, (3) modern remote sensing technologies such as UAV and LiDAR, and (4) GIS-based methods, spatial analysis, and artificial intelligence. This study concludes that coastal change can be tracked using any form of remote sensing, including drones, LiDAR, higher resolution imaging, and Landsat imagery. This review provides a comprehensive reference for upcoming work on coastal management and exploitation development and research, especially for the low elevation coastal zones that are affected by coastal hazards.

Keywords: Coastline changes; Coastal erosion; Coastal hazards; Coastal vulnerability assessment; Remote sensing.

INTRODUCTION

The boundary between the land and the sea is represented by coastal zones. It has less coverage than 20% of the Earth's land surface; however, nearly half of the world's population lives next to the coasts of oceans and seas (Mentaschi *et al.,* 2018; Crossland *et al.,* 2005). Over 1.6 million kilometers of coastline exist worldwide, and 84% of all countries have coasts (either with inland waters, open oceans, or both) (Melet *et al.,* 2020). The shoreline, delineating the interface between land and sea, serves as a fundamental indicator of environmental shifts, reflecting alterations in coastal conditions, including fluvial processes, sediment supply, and relative sea level. It stands out as one of the highly dynamic coastal geomorphological features (Cabezas-Rabadán *et al.,* 2015). The positions of coastlines change dramatically in response to several natural and anthropogenic factors, including climate change, waves and currents, sea level rise, storm surges and hurricanes, and human activities (Dewi and Bijker, 2020).

Climate change has significant impacts on shorelines, leading to a phenomenon known as shoreline retreat. Shoreline retreat refers to the gradual movement of a coastline away from its previous position. Several factors associated with climate change contribute to this phenomenon, including sea level rise, increased storm intensity, melting ice and permafrost, and loss of coastal habitats. Approximately 30% of the global coastline consists of sand and mud deposits, including river deltas, which are more susceptible and vulnerable to coastal erosion processes than rocky and protected coasts (Luijendijk *et al.,* 2018). Previous studies have indicated that nearly 80% of global coasts are in the process of eroding at rates up to 10 m/yr. which threatens coastal infrastructures, natural resources, coastal tourism, archaeological sites, and sustainable coastal planning goals (Pilkey and Hume, 2001; Younis *et al*., 2014; Darwish 2023). Recently, remote sensing-based spatiotemporal mapping of coastlines has been increasingly utilized for navigation, protection, and coastal management applications (Di *et al.,* 2003; Liu and Jezek, 20014; Li and Damen, 2010).

The availability of continuous monitoring of coastal zones using satellite remote sensing time series has helped in tracking and quantifying coastal changes. Coastline changes are influenced by a variety of natural and human-induced factors. These factors can interact in complex ways, leading to dynamic changes in coastal landscapes, including wave, tidal and siltation action (Wu and Hou, 2016; Moore *et al.,* 2013), currents (Williams and Kraus, 1999), hurricanes and cyclones (Xu, 2018), and sea level rise (List *et al.,* 1997; Zhou *et al.,* 2013). However, human activities along coasts contribute to coastline changes by urbanization and residential housing construction,

* *Corresponding author e-mail: kamal.srogy@mu.edu.eg*

seawalls, groins, jetties, harbor dredging, sea enclosures and reclamation, harbor construction, and fishpond construction (Zhang *et al.*, 2015; Wu *et al.*, 2022; AI *et al.*, 2019). River damming is also considered one of the most critical anthropogenic factors affecting sediment supply, which feeds the deltas coasts (Darwish *et al.*, 2017).It is estimated that coastal areas lost approximately 28,000 sq. km between 1984 and 2015, which is twice as much as the land gained over the same period (Mentaschi *et al.*, 2018). In the United States (US), coastal property losses cost billions of dollars (U.S., 2022a). The US spends millions of dollars annually on beach nourishment, seawall construction, groin construction, and other coastal protecttion devices (U.S., 2022b; Li and Gong, 2016; Xu and Gong, 2018; Wu *et al.*, 2014). In Egypt, the anticipated expenditure for constructing the sea wall along the northern coast is projected to be $1.0 billion for a length of 1,000 km (Abd-Elhamid *et al.*, 2015).

The integration of remote sensing datasets and geographic information system (GIS) techniques has increased for coastline change analysis and quantification along different continental coasts due to recent progress in geospatial technologies. Along most of the world's coastal regions, the dynamics of coastlines are observed and evaluated through the extensive application of multisource remote sensing datasets and geographic information systems technologies.

The study of collecting information about objects or locations from a distance, usually using aircraft or satellites, is known as remote sensing. By identifying the energy that is reflected from Earth, remote sensors acquire data. Both passive and active forms are possible. Remote sensing is being increasingly utilized in coastal applications to map coastal geomorphic characteristics, track sediment movement, and monitor changes to coastlines. Furthermore, satellite information can be utilized to minimize erosion and map coastal areas (NOAA, 2022).

Numerous studies have attempted to examine this topic and determine the most effective method based on a number of computations and algorithms. To identify coastal features and patterns, image classification methods and spectral indices were also applied to satellite imagery. Over the past 20 years, a wide range of numerical techniques, factors, and algorithms have been developed and used on a number of data formats, including satellite and aerial photographs, optical and radar data, and the most recent high-resolution images from unmanned aerial vehicles (UAVs).

In this study, an analysis of the most recent techniques and methods, progress and future trends of coastline delineation and automatic extraction from remotely sensed data as well as GIS methods for coastline quantification and spatiotemporal analysis was performed. To achieve the objectives of this study, eighty-three global published studies in top indexed journals that utilized satellite remote sensing images and GIS techniques from 2012 to 2022 were collected, as shown in Figure (1).

Additionally, the literatures collected, concerned coasts and shoreline detection methods, were classified into four parts: i, long-term coastline changes as shown in Table (1); ii, short-term coastline changes, presented in Table (2), iii, climatological and anthropological impacts on coastline changes shown in Table (3), and iv, remote sensing and GIS methods displayed in Table (4). The rest of this review provides a state-of-the-art review of coastline detection methods used in optical and radar remote sensing as well as GIS-based statistical computational techniques.

Coastline Definition

The coastline is widely recognized as a highly dynamic boundary between water and land surfaces, making it an important indicator of morphological trends (DaSilva *et al.*, 2021). An essential component of Integrated Coastal Zone Management (ICZM) is the monitoring of the coastline location and the elements that influence coastal dynamics at multiple levels (Bruno *et al.*, 2016). For the purpose of continuous beach monitoring and maintaining its functions of protection, recreation, and natural values, the shoreline position is very helpful in quantifying historical erosion rates and beach width and volume.

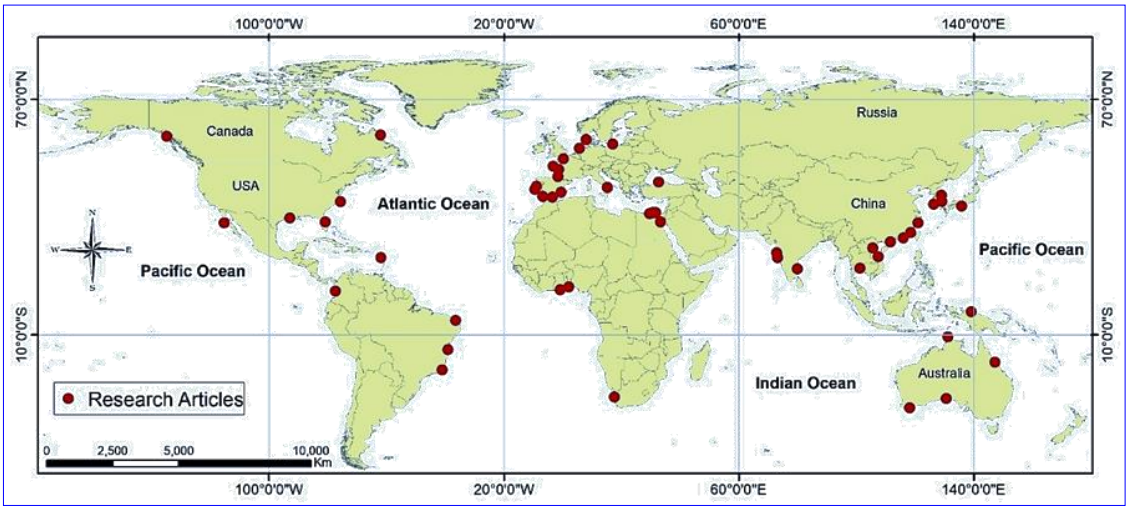

Figure (1): Geographical distribution of the literature described in this study.

Table (1): Long-term coastline dynamics: Comparative analysis of costal studies and data extraction methods.

Authors/publication year	Time Period covered	Studied Location	Data Input	Extraction methods and Analysis
Chaaban *et al*., (2012)	1946-2005	France	Aerial Photographs	Digitizing, ArcGIS® Modelbuilder
Pardo-Pascual *et al.*, (2012)	1984-2010	Spain	Landsat Imagery	Automatic, Subpixel
Bayram *et al.*, (2013)	1986-2009	Turkey	Landsat Imagery	Digitizing, Shoreline and LULC)
Cenci *et al.*, (2013)	1984-2011	Portugal	Landsat Imagery	DVI threshold, GIS-based DSAS
Ford *et al.*, (2013)	1945-2012	Marshall Island	Aerial Photographs HR Images	Digitizing, GIS-based DSAS
Aps *et al.*, (2014)	1995-2012	Spain	Landsat Imagery	Semiautomatic, ESI, Internet GIS technologies
El-Asmar *et al*., (2014)	1973-2011	Egypt	Landsat, SPOT, and Egysat-1	Digitizing, Change Detection
Kaiser (2014)	1990-2005	Egypt	Landsat Imagery	Digitizing, GENESIS Model
Puig *et al.*, (2014)	1956-2010	Spain	Aerial Photographs	Digitizing, GIS-based DSAS, Storm analysis
Suo and Zhang (2015)	1990-2010	China	Landsat Imagery	Semiautomatic, Coastline Tortuosity Index
Adnan *et al.*, (2016)	1987-2011	Australia	Aerial Photographs	Semiautomatic, Edge of Vegetation Line (EVL)-GIS-based DSAS
Bruno *et al*., (2016)	2009-2015	Italy	SAR	COSMO-Beach
Li and Gong (2016)	1984-2013	USA	Landsat Imagery	Semiautomatic, AWEI Index
Darwish *et al.*, (2017)	1945-2015	Egypt	Landsat Imagery	Semiautomatic NDWI, MNDWI, GIS-based DSAS
Evadzi *et al.*, (2017)	1974-2015	Ghana	Landsat, DEM, TOPEX/Poseidon	Semiautomatic, WLR, OLS, GIS-based DSAS
Sagar *et al.*, (2017)	1987-2015	Australia	Landsat Imagery	Semiautomatic, NDWI, GPS RTK
Collin *et al*., (2018)	1969-2013	France	Aerial Photographs, Pleiades-1	Digitizing, DSAS Bathymetry modelling
Li et al., (2018)	1974-2014	China	Landsat Imagery	Semiautomatic Extract, NDWI, GIS
Paniagua-Arroyave *et al.*, (2018)	1938-2009	Caribbean	Aerial Photographs	Mapping Cliff-retreat, GIS-based DSAS
Wang *et al.*, (2018)	1986-2016	China	Landsat, GEE	Semiautomatic, NDVI , EVI, LSWI, MNDWI
Chaumillon *et al.*, (2019)	1840-2016	France	Aerial Photographs, Satellite Images.	Digitizing, DSAS, Topographic profiles
Do *et al.*, (2019)	1985-2010	Holland	Landsat, LIDAR	JARKUS-derived shoreline
Jolivet *et al.*, (2019)	1955-2017	Amazon	Aerial Photographs Satellite Images	GIS –based DSAS
Robin *et al.*, (2019)	1950-2011	France	Aerial Photographs	Digitizing,Beach/Dune Shoreline
Stéphan *et al.*, (2019)	1949-2009	France	Aerial Photographs	Digitizing, GIS-based DSAS
Cao *et al.*, (2020)	1985-2017	China	Landsat, GEE	Semiautomatic, MNDWI
Carvalho and Guerra (2020)	1986-2018	Brazil	Landsat Imagery	GIS-based CVI, Natural and Social
Diniz *et al.*, (2020)	1984-2017	Brazil	Landsat Imagery	GNSS GPS, PPK
Li *et al.*, (2020)	2002-2018	China	Landsat Imagery	Semiautomatic, NDWI, ELPC Model
Liu *et al.*, (2020a)	1985-2017	China	Landsat Imagery	Semiautomatic, GIS analysis
Liu *et al.*, (2020b)	1976-2017	China	Landsat Imagery	Semiautomatic, GIS-DSAS
Lymburner *et al.*, (2020)	1987-2016	Australia	Landsat, Digital Earth	Semiautomatic, NDVI
Reshma and Murali (2018)	1973-2014	India	Landsat	Semiautomatic
Song *et al.*, (2020)	2000-2015	Southeast Asia	Landsat, Google Earth, HR Imagery	Semiautomatic, GIS-DSAS
Abdurrahman *et al*., (2021)	1996-2020	Indonesia	Landsat, Google Earth	Semiautomatic, DSAS
Balle *et al.*, (2021)	1988-2018	Benin	SPOT and Sentinel-2	Detect High-Water Line, DSAS
Bishop-Taylor *et al.*,(2021)	1988-2019	Australia	Landsat Imagery	Semiautomatic, MNDWI
DaSilva *et al.*, (2021)	1975-2017	Australia	Aerial, RapidEye	Semiautomatic, GIS-DSAS
Kim *et al*., (2021)	1980-2017	Korea	Aerial Photographs	Modelling Approach
González Rodríguez *et al.*, (2021)	1780-2018	Colombia	Google Earth	AutoCAD
Teixeira *et al*., (2021)	1988-2019	Brazilian	Landsat Imagery	Erosion Geoindicators, ENVI 5.5
Yun *et al*., (2021)	1986-2020	South Korea	Aerial Images, UAV's	Semiautomatic, GIS-DSAS
Renard *et al.*, (2022)	1950-2017	Guadeloupian	High-Resolution, Aerial Photography	Semiautomatic, GIS-DSAS
Yang *et al.*,(2022)	1986-2020	NE US	Landsat Imagery	NDVI, MNDWI, DECODE

Table (2): Short-term Coastline Dynamics Studies: Comparative analysis of costal studies and data extraction methods.

Authors/ publication year	Time Period covered	Location	Data Input	Coastline Extraction method and Analysis
Aly *et al.* (2012)	1993-2000	Egypt	InSAR	Digitizing, Remote Sensing, Image Processing
Araújo *et al.*, (2014)	2011	Portuguese	LiDAR	Automatic, GENESIS
Paine *et al.*, (2017)	2010-2012	Texas	LIDAR	Automatic, GIS-Based DSAS
Nijland *et al.*, (2017)	2012	Canada	LIDAR	Semiautomatic
Kim *et al.*, (2017)	2010-2013	Korea	Airborne LiDAR Bathymetry	GIS, Video Monitoring; Geospatial Information of 3D Point Cloud Data
Le Bas and Levoy (2018)	2011-2017	France	LiDAR	Semiautomatic, GIS-Based DSAS
Terefenko *et al.*, (2018)	2016-2017	Poland	LiDAR	COAMPS
Kim *et al.*, (2018)	2016	Korea	LiDAR	RTK-GNSS
Stéphan *et al.*, (2019)	2006-2009	France	Aerial Photographs	Semiautomatic
Waghmare *et al.*, (2020)	2016-2017	India	Sentinel-2A	GIS-Based DSAS- Subtraction of Images
Wang *et al.*, (2020)	2014-2018	China	Landsat Imagery	Semiautomatic Water Edges Extracted
Al-Aesawi *et al.*, (2020)	1971-2016	Shatt Al-Arab	Landsat and Admiralty maps	DSAS, Geo informatics Analyses, ERDAS Imagine

Table (3): Climate and Anthropogenic Impacts of Coastline Dynamics Studies:.

Authors/ publication year	Time Period covered	Location	Data Input	Coastline Extraction method and Analysis
Puig *et al.*, (2014)	1956-2010	Spain	Aerial Photographs O	Digitizing DSAS, Storm analysis
Hereher (2015)	2015	Egypt	Landsat Imagery	Manual GIS-based CVI, Climate Change
Albuquerque *et al.*, (2018)	2016	Brazil	UAV's	Meteo-Oceanographic Events
Kang *et al.*, (2018)	2012	Korea	IPCC, SLR	Disaster Impact Index (CDII), GIS, Storms
Ritphring *et al.*, (2018)	Up-to-2100	Thailand	IPCC	Projections of Future, GIS, Sea Level Rise
Terefenko *et al.*, (2018)	2016-2017	Poland	LiDAR	Storm analysis
Carvalho and Guerra (2020)	1986-2018	Brazil	Landsat Imagery	GIS-CVI, Natural and Social Impacts
Kelly and Gontz (2020)	2019	Australia	LIDAR, Planet Scope	DSAS, Tropical Cyclone Oma
Nagdee *et al.*, (2020)	1973-2004	Barbados	Aerial Photographs	DSAS, Hurricanes Allen1980, Ivan 2004
Wang *et al.*, (2020)	2018	Florida	Airborne LIDAR	Storm Wave Generated, Hurricane Michael
Thakare *et al.*, (2021)	1973-2019	India	Landsat, ASTER	ERDAS IMAGINE ArcGIS- CVI
Peng *et al.*, (2021)	2008–2016	Australia	Satellite altimeter Jason-1	Sea Level Rise
Balstrøm and Kirby (2022)	2007-2015	Denmark	Digital Terrain Model	DHyMSea, Esri's ArcGIS Pro
Jose and Carlin (2022)	2004	Florida	LIDAR, Google Earth	Storm- Hurricane Season
Youn and Zarillo (2022)	1972-2013	Korea	Google Earth	Digitized Orthogonal Lines, Typhoons Flooding

Table (4): Comparative Analysis of Coastal studies and data extraction techniques for Coastline mapping.

Authors/ publication year	Location	Data Input	Coastline Mapping	Methods
Luque *et al.*, (2012)	Spain	LiDAR	Automatic	Automatic Vertical Datum
Guastella *et al.*, (2014)	S. Africa	Google Earth	Digitizing	No Data
Hereher (2015)	Egypt	Landsat Imagery	Semiautomatic	CVI
Hsiao *et al.*, (2016)	China	Satellite Altimetry, HR imagery	Digitizing	No Data
Gerrity *et al.*, (2018)	San Mateo	Google Earth Images	Semiautomatic	CVI
Jun *et al.*, (2018)	Korea	Drone Terrestrial LiDAR	3D DSM CAD	Drone (UAV), Pix4Dmapper
Kim *et al.*, (2018)	Korea	Mobile LiDAR	Automatic	RTKGNSS
Wozencraft *et al.*, (2018)	USA	LiDAR, High-Resolution Aerial Imagery	Semiautomatic	GIS Spatial Index
Dai *et al.*, (2019)	USA	Quick Bird, GeoEye-1, WorldView-2	Semiautomatic	"NDWI, SAM, Automated Water Extraction Index (AWEI)"
Nijland *et al.*, (2019)	Canada	Landsat Imagery, GEE WorldView-2	Semiautomatic	NDVI
Poitevin *et al.*, (2019)	France	Space-Borne Geodetic Methods, In SAR, GPS	Semiautomatic	Vertical Land Motion & Relative Sea-Level Changes
Fan *et al.*, (2020)	China	Landsat, LiDAR	Automatic	GIS
Jaramillo *et al.*, (2020)	Indonesia	Aerial Photographs	Video-Camera, Satellite Images	Subpixel Technique, SHOREX algorithm
Tak *et al.*, (2020)	Korea	Drone, Terrestrial LiDAR	Semiautomatic	RTK GPS, Drone, CCTV, Digital Surface Model (DSM)
Hossain *et al.*, (2021)	China	IKONOS	Semiautomatic	Fuzzy Shoreline Map
Zhao *et al.*, (2021)	-	Point Cloud, LIDAR	W/L Discriminator	Point Cloud Clustering
Mao *et al.*, (2022)	World	SRTM, GEE)	Vector coastline Open Street Map	Indices, Machine Learning
Seale *et al.*, (2022)	World	Sentinel-2, Landsat, GEE	Automatic, Water Edges	Deep Learning CNN, QGIS

Shoreline management is essential for navigation, coastal resource management, and coastal planning and development (Arnous *et al.*, 2022). Understanding the complexities of coastal dynamics is essential for effective coastal management and sustainable development.

Coastline Types and Indicators

Geology is the essential factor influencing coastline dynamics. There is no similar response of silty, sandy, biological, rocky and artificially protected shores to coastal processes, climate change and anthropogenic activities. Shoreline indicators are crucial in assessing the impacts of climate change on coastal areas. Changes in shorelines can be indicative of various climate-related processes, including sea level rise, increased storm intensity, and alterations in precipitation patterns. In this study, different types of coasts were analyzed around the world, such as sandy coasts in the southern and northern Shandong Peninsula in China (Yue *et al.,* 2021), the silty Nile Delta coast between 1945 and 2015 (Darwish *et al.,* 2017), and Brittany sandy/gravel beaches in western France (Stéphan *et al.,* 2019). The coral reefs coast along Atoll reef islands along Takapoto Atoll in French Polynesia (Collin *et al.,* 2018). Modifications of coastlines can cause damage to coastal resources, such as coastal mangroves along the Egyptian Red Sea coast (Moustafa *et al.,* 2023) and coral reefs at Moorea Island, French Polynesia (Gasc *et al.,* 2021). The rocky cliff retreat occurs along the western coast along the Caribbean coast of Colombia (Paniagua-Arroyave *et al.,* 2018). The coastal changes along the Artificially protected coastline of the South Korean coastline were analyzed between 1970 and 2010 (Lee *et al.,* 2020).

Multispectral Imagery for Shoreline Monitoring

Coastal environmental change has been continuously observed using optical remote sensing satellites with moderate and high spatial resolutions. When compared to field surveys, remote sensing has been shown to be an effective means of tracking coastal dynamics across a range of spatial scales. One of the main benefits of satellite remote sensing images is their global coverage, which includes frequent coverage of most coasts in all seasons and climates. However, because public resolution is too coarse to offer information on most coastal morphodynamic changes, mid-resolution satellite images have been overlooked.

Satellite-Remote Sensing Imaging Systems

Refer to the technology and instruments used to capture information about Earth's surface, atmosphere, and oceans from space. These systems utilize satellites equipped with various sensors to collect data in the form of images or other measurements. Medium-resolution satellite imagery has been widely used in several studies to assess and map coastline dynamics along the world's coasts. Landsat imagery has been the main data source for many coastal studies from 1972 to now (Pardo-Pascual *et al.,* 2012; Bayram *et al.,* 2013; Cenci *et al.,* 2013; Aps *et al.,* 2014; El-Asmar *et al.,* 2014; Kaiser, 2014; Hereher, 2015; Suo and Zhang, 2015; Li and Gong, 2016; Evadzi *et al.,* 2017; Darwish *et al.,* 2017; Sagar *et al.,* 2017; Li *et al.,* 2018; Wang *et al.,* 2018; Do *et al.,* 2019; Nijland *et al.,* 2019; Al-Aesawi *et al.,* 2020; Carvalho and Guerra, 2020; Cao *et al.,* 2020; Diniz *et al.,* 2020; Fan *et al.,* 2020; Lymburner *et al.,* 2020; Reshma and Murali, 2018; Li *et al.,* 2020; Liu *et al.,* 2020; Song *et al.,* 2020; Abdurrahman *et al.,* 2021; Bishop–Taylor *et al.,* 2021; Thakare and Shitole, 2021; Yang *et al.,* 2022). As the spatial resolution of Landsat improved with new generations of satellite sensors, researchers found it to be an increasingly useful tool for assessing coastal changes. On the other hand, Sentinel imagery, with a 10 m foot-print, was used to extract coastal features using the high-water line (Balle *et al.,* 2021; Waghmare *et al.,* 2020). SPOT-4 images taken between 2006 and 2011 were used to quantify coastline changes along the Damietta promontory coast in Egypt (El-Asmar *et al.,* 2014).

High-resolution satellite imagery, such as worldview and IKONOS imagery, has become very common for coastline mapping and change detection applications (Hossain *et al.,* 2021). It was used for assessing coastal dynamics in several locations around the world, including the Marshall Islands in France, the Colombian coasts and the Chinese coasts (Ford, 2013; Giraud-Renard *et al.,* 2022; Hsiao *et al.,* 2016). IKONOS (Hossain *et al.,* 2021), PlanetScope (Kelly and Gontz, 2020), Pleiades-1 (Collin *et al.,* 2018), RapidEye (DaSilva *et al.,* 2021), QuickBird, Worldview-2 (Dai *et al.,* 2019; Nijland *et al*., 2019), and high-resolution Google Earth imagery were used to study coasts in Indonesia, Colombia, Korea, USA and South Africa (Abdurrahman *et al.,* 2021; González Rodríguez *et al.,* 2021; Youn and Zarillo, 2022; Guastella *et al.,* 2014; Gerrity *et al.,* 2018). IKONOS imagery, with a footprint of one meter, was used to map coastlines of the South China Sea (Hossain *et al.,* 2021). The high spatial and temporal resolution of Planet Scope imagery enabled mapping of the high-water line (Kelly and Gontz, 2020).

Non-Satellite Imaging Systems

Non-satellite imaging systems refer to technologies and instruments that capture images or data about the Earth's surface, atmosphere, or other targets without relying on satellites. These systems are often ground-based or airborne, and they serve various purposes in fields such as research, surveillance, monitoring, and industry. Aerial photographs are considered one of the most valuable and accurate geospatial data used to assess and map the historical changes in coastlines since the 1930s. Coastlines were manually traced from aerial photographs taken in 1945 along the Marshall Islands in the Pacific Ocean (Ford, 2013). Chaaban *et al.* (2012) assessed coastal changes in northern France based on aerial missions that began in 1946 and lasted until 2005. Tracing of aerial photographs was used to assess rising sea level along Wotje Atoll in the Marshall Islands (Ford, 2013). Other examples have used aerial photographs to detect coastal changes, including North Keeling Island in Australia (1987-2011) (Adnan *et al.,* 2016), (1938-2009) along the Caribbean Coast of Colombia (Paniagua-Arroyave *et*

al., 2018), Takapoto Atoll in France (1969-2013) (Collin *et al.*, 2018), (1840-2016) (Chaumillon *et al.*, 2019), (1949-2009) along the Brittany Coast in northern France (Stéphan *et al.*, 2019), and (1975-2005) along Cape Jaffa, South Australia (DaSilva *et al.*, 2021). Moreover, aerial photographs were widely used to assess the impacts of extreme climatic events such as hurricanes along the Barbados coast in the Caribbean Sea between 1973 and 2004 (Nagdee *et al.*, 2020). Furthermore, the integration of aerial photographs with other spatial data sources was used to assess shoreline evolution and surface changes along the Pays de la Loire coast in western France (1950-2010) (Robin *et al.*, 2019).

Drones can deploy all forms of remote sensing, including multispectral scanners, LiDAR, thermal infrared, digital photography and RADAR. Drones have been used in several studies of coastal dynamics (Yun *et al.*, 2021; Giraud-Renard *et al.*, 2022; Albuquerque *et al.*, 2018; Wozencraft *et al.*, 2018). The combination of historic digitized aerial photographs taken in 1986 with drone-based digital imagery taken in 2020 was used to map coastline changes at Chollipo Beach in South Korea (Yun *et al.*, 2021). Video monitoring systems are ground-based cameras that have been recently used to accurately monitor beach erosion and shoreline changes along different coasts worldwide (Arriaga *et al.*, 2022).

Coastline Extraction Techniques and Mapping

The utilization of geographic information science and remote sensing technology has increased globally in the last decade for coastline extraction, mapping and assessment of morph dynamics over short and long time periods. Different techniques and methods for coastline delineation were selected from the literature analysis.

Manual Shoreline Delineation

It is the first delineation method for coastline mapping from aerial photographs and topographic maps (Chaaban *et al.*, 2012; Ford, 2013). Manual digitizing of a coastline is tedious and subject to interpretation error. It is particularly difficult to delineate the coastline from wet sand in clear shallow water. Therefore, several methods to automatically extract coastlines from ocean edges have been developed. Figures (2) and (3) show examples of coastline mapping over time.

Remote Sensing Indices Semiautomatic Shoreline Extraction

This approach has been applied in several studies (Sagar *et al.*, 2017; Darwish *et al.*, 2017; Cao *et al.*, 2020). Spectral indices were used to differentiate coastlines from satellite images; the normalized diff-erence water index (NDWI), modified normalized difference water index (MNDWI), automated water extraction index (AWEI), and other indices were applied to identify coastlines. Water index calculated as follow:

$$\mathrm{NDWI} = \frac{(\rho_{\mathrm{Green}} - \rho_{\mathrm{NIR}})}{(\rho_{\mathrm{Green}} + \rho_{\mathrm{NIR}})}$$

Where, ρGreen, is the top-of-atmosphere of the green band and ρNIR, is that of the near infrared band.

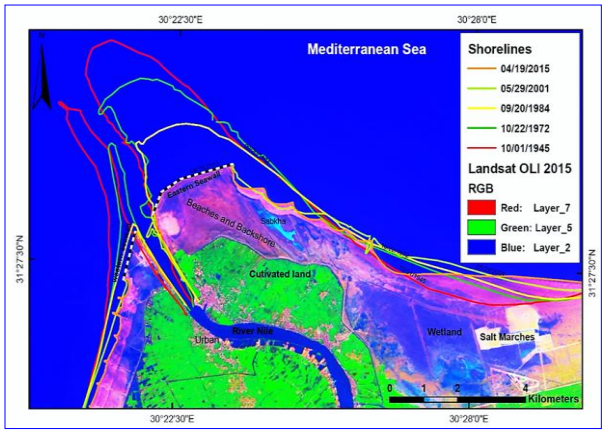

Figure (2): Rosetta Promontory in Egypt Retreating Between 1945 (Surveyed) and 2015 (Landsat), After (Darwish *et al.*, 2017).

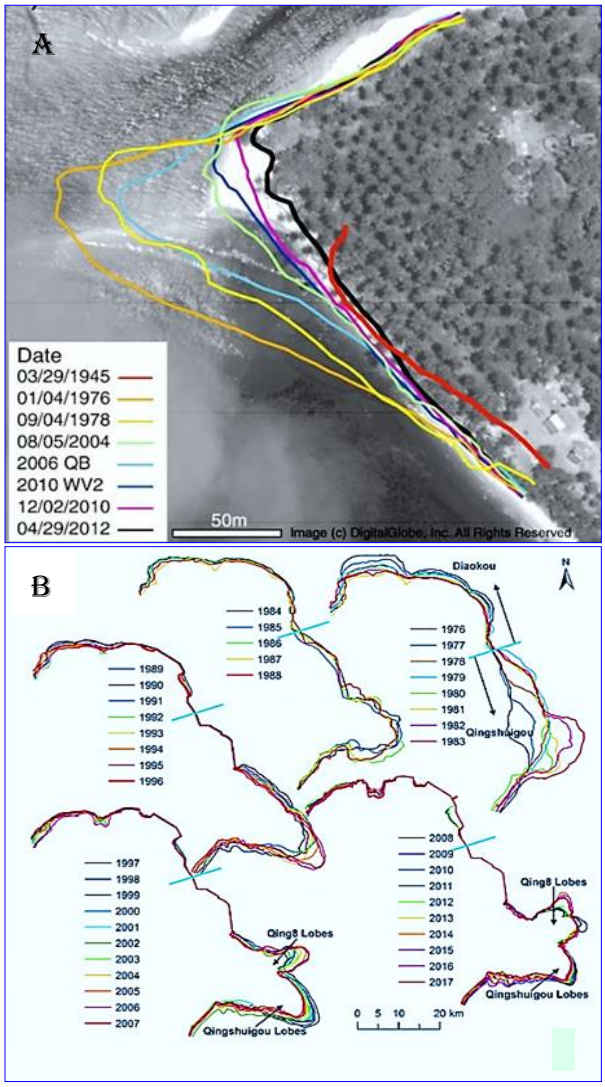

Figure (3): Semi-Automatic Coastline mapping along a) Marshall Islands in France Between 1945 and 2012 using Aerial Photographs, Landsat, and Quick bird Imagery, After (Ford, 2013). B) Yellow River Delta Coastline Changes (1976–2017) after (Liu *et al.*, 2020).

Water bodies are expected to yield a positive NDWI, while, modified normalized difference water index (MNDWI) was calculated as follow:

$$\mathrm{MNDWI} = \frac{\rho_{\mathrm{Green}} - \rho_{\mathrm{MIR}}}{\rho_{\mathrm{Green}} + \rho_{\mathrm{MIR}}}$$

The normalized difference vegetation index (NDVI) and enhanced vegetation index (EVI) were used to differentiate tidal flats from open water between high and low water lines (Wang *et al.*, 2018) . Several studies have used the NDVI and EVI indices for mapping water bodies and vegetated coastal areas (Lymburner *et al.*, 2020; Wang *et al.*, 2018; Yang *et al.*, 2022; Nijland *et al.*, 2019). The EVI was calculated as follow:

$$EVI = 2.5 \times \frac{\rho_{nir} - \rho_{red}}{\rho_{nir} + 6 \times \rho_{red} - 7.5 \times \rho_{blue} + 1}$$

Where, ρblue (450–520 nm), ρgreen (520–600 nm), ρred (630–690 nm), ρnear-infrared (NIR: 760–900 nm).

The spectral algorithm of NDVI was utilized to distinguish between water, beach and vegetation. The land surface water index (LSWI) is hyper-sensitive to both soil moisture and plant water content. It is computed by averaging the ratio within the near-IR and shortwave infrared bands (Wang *et al*., 2018).

The NDVI algorithm and The land surface water index (LSWI) were calculated as follow:

$$NDVI = \frac{\rho_{nir} - \rho_{red}}{\rho_{nir} + \rho_{red}}$$

$$LSWI = \frac{\rho_{nir} - \rho_{swir}}{\rho_{nir} + \rho_{swir}}$$

Where, ρshortwave infrared (SWIR: 1550–1750 nm) bands of Landsat TM/ETM+/OLI imagery were used.

Automated Water Extraction Index (AWEI)

This index provides a higher accuracy and the most stable threshold to classify pixels at the edge of the water surface (Dai *et al.*, 2019) and calculated as:

$$AWEI = 4 \times (\rho_2 - \rho_5) - (0.25 \times \rho_4 + 2.75 \times \rho_7)$$

Where, ρ represents the surface reflectance value of spectral bands of Landsat TM/ETM+ imagery (Li and Gong, 2016).

Automatic Coastline extraction using edge detection

Detection of high-water lines using spatial filtering is a very important approach for automatic shoreline mapping and has been utilized by several researchers (Paravolidakis *et al.*, 2018; Balle *et al.*, 2021; Adnan *et al.*, 2016).

Sea-land segmentation (SLS)

Sea-land segmentation of remote sensing images is of great significance to the dynamic monitoring of coastlines (Cui *et al.*, 2021). The goal of sea-land segmentation (SLS) is to map and isolate the land and sea zones from coastal remote sensing imagery (Aghdami-Nia *et al.*, 2022). In numerous coastal and environmental studies, such as coastline extraction, coastal erosion analysis, coastal area monitoring, and ship or iceberg identification, sea-land segmentation (SLS) plays a vital role in remote sensing activities.

Polarization Methods for SAR Data

Coastline extraction using SAR data involves the interpretation of radar backscatter responses from various surfaces. Different polarization methods provide varying sensitivities to surface characteristics, allowing for the discrimination of water, land, and other features. Integrating polarization information with other SAR image processing techniques enhances the accuracy of coastline extraction and supports applications such as environmental monitoring, change detection, and disaster response in coastal areas. This approach was used by several studies to detect the coastline for change analysis in different locations worldwide; Bruno *et al.* (2016) applied it in Italy, Aly *et al*. (2012) applied it in Egypt, and Poitevin *et al.* (2019) used this approach in France for sea level change analysis.

Change Detection

The use of digital image processing has increasingly utilized for coastal environmental change, land use cover change and integrated coastal zone management. Both pixel and post classification techniques were applied to assess the influence of land use change, urbanization, coastal protection works and coastline dynamics. Murali *et al.* (2020) applied a spatiotemporal change detection approach to assess changes in the Godavari Delta region on the east coast of India between 1973 and 2019. Abualtayef *et al.* (2021) applied a change detection approach for assessing the Gaza coast between 2004 and 2016 using SPOT-5, Landsat and Quick Bird and GIS tools.

Image Classification

Satellite image classification for coastline change detection involves using machine learning and image processing techniques to analyze satellite imagery and identify changes in the coastal area over time. The goal is to classify different land cover types and detect alterations in the coastline due to factors such as erosion, accretion, or human activities. The classify-cation makes a boundary between land and sea, which is the coastline (Abdurrahman *et al.*, 2021). The subpixel classification technique is a high-precision geometric method for automated shoreline detection from Landsat TM and ETM$^+$ imagery. The method-ology is based on the application of an algorithm that ensures accurate image geometric registration and the use of a new algorithm for subpixel shoreline extra-ction (Ford, 2013). The subpixel shoreline acquisition method (SHOREX algorithm) was used to assess shoreline evolution using satellite-derived shorelines (Jaramillo *et al.*, 2020).

Coastline Uncertainty and Positional Accuracy Assessment

The uncertainty in the shoreline's position involves potential location errors. It is equal to the square root of the sum of squared errors, is expressed in meters (m), and can be measured from three sources of error; the first source is the aerial pixel size. The second is the precision of the orthorectification or georeferencing process (RMS errors) which can be calculation as the equation:

$$RMSE = \sqrt{\frac{\sum_{i=1}^{t} (D_{r,i} - D_{x,i})^2}{t}}$$

Where, the distance that exists between the baseline and the obtained coastline at transect i is

denoted by D(x,i), the distance that is linear between the baseline and the reference coastline at transect i is represented by D(r,i), and the total number of transects is represented by t.

The accuracy of manually digitizing shorelines comes last (Robin *et al.*, 2019). Surveying maps and aerial photographs were employed to evaluate seven causes of uncertainty concerning the shoreline's position, five of which are appropriate for aerial photographs: errors related to pixels, rectification, digitization, seasonality, and tidal fluctuation (Ford, 2013) with the following equation:

$$ESP(m) = (Ep^2 + Eo^2 + Ed^2)^{0.5} \text{and } EPS^2(m^2) = EPS^*25$$

Where, Ep is the error pixel, Eo is the RMS error (m), Ed is the error digitizing (m), and EPS is the shoreline position uncertainty (m) as done by Robin *et al.*, (2019).

The uncertainty in the reference position of the shoreline was estimated using aerial photos that were used as base material for georeferencing at the subpixel level (Pardo-Pascual *et al.*, 2012). The RMSE was calculated for uncertainty analysis (Li and Gong, 2016). The most effective method of checking the uncertainty in the precise position of the coast is through RTK-GPS surveying (Sagar *et al.*, 2017).

GIS-Based spatial computation of coastline change

The digital shoreline analysis system (DSAS) is one of the most broadly utilized techniques for the analysis of such studies in the world. The Digital Shoreline Analysis System (DSAS) is a GIS-based system established by the USGS. It calculates gaps among the coastline positions during defined periods. DSAS 5.0 statistical methods include net shore movement (NSM) related to date, and only two shorelines require the total distance between the earliest and the latest coastline in each transect. The end point rate (EPR) statistical parameter describes the spatial patterns of shoreline change. EPR measures shoreline change by dividing the distance of the coastline between its initial and the most current position of coastline as followed:

$$EPR = \frac{\text{Distance}}{\text{Time}} = \frac{\text{Net Shoreline Movement(m)}}{\text{Time Span(Years)}}$$

The long-term rate of variation is determined through a linear regression rate (LRR), which integrates the current data. In the present study, several studies used DSAS for the quantitative assessment of coastline dynamics (Cenci *et al.*, 2013; Puig *et al.*, 2014; Darwish *et al.*, 2017, Jolivet *et al.*, 2019; Al-Aesawi *et al.*, 2020; Kelly and Gontz, 2020; Darwish and Smith, 2021; Darwish and Smith, 2023) (Figure 4).

The automated extraction of coastlines using various pixel and subpixel techniques, along with an uncertainty assessment of the extracted coastlines and the calculation of the end point rate (EPR), is demonstrated. Figure (5) illustrates the perpendicular techniques employed in DSAS for coastline change analysis in various global locations. GIS-based shoreline prediction modeling involves the use of geographic information systems (GIS) to develop models that predict changes in shoreline positions over time.

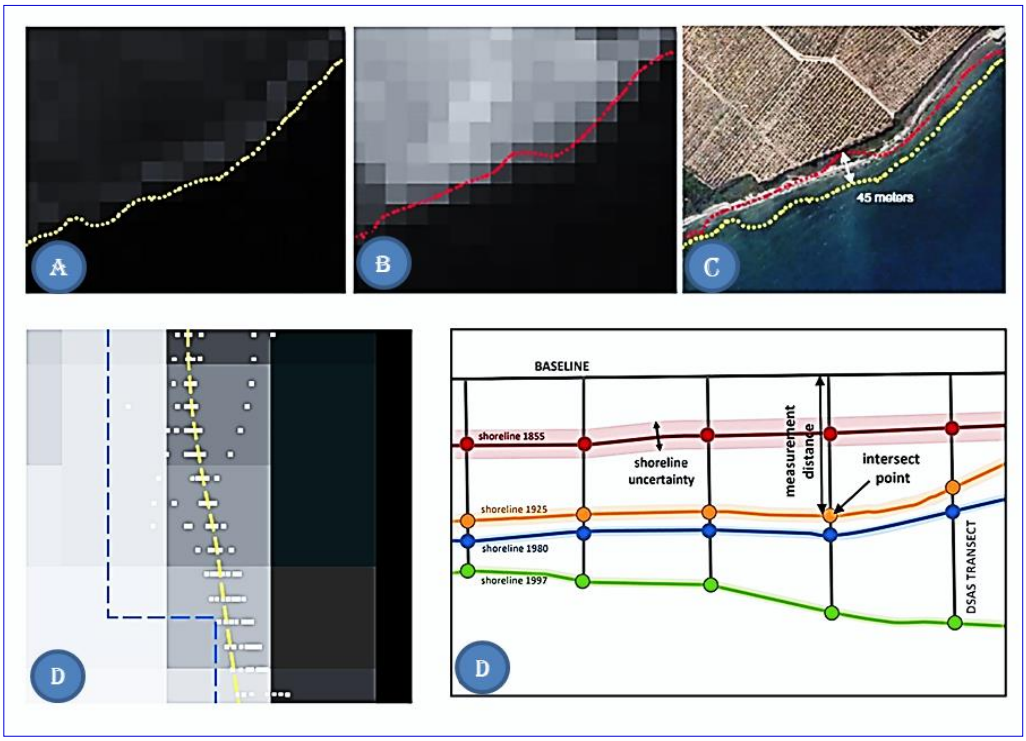

Figure (4): Subfigures (a,b,c) show automatic shoreline extraction at different pixel and subpixel techniques, d) show positional accuracy assessment of automatic extracted shorelines (after (Pardo-Pascual *et al.*, 2012), and e) DSAS based spatial computational techniques, after https://www.usgs.gov/centers/whcmsc/science/digital-shoreline-analysis-system-dsas.

These models are valuable tools for coastal management, environmental planning, and risk assessment. Shoreline prediction provides a comprehensive approach to understanding and managing coastal environments. It helps stake-holders anticipate future changes, assess risks, and implement strategies to mitigate the impacts of coastal dynamics.

Artificial Intelligence

Artificial intelligence (AI) has the potential to significantly enhance coastal change assessment by automating processes, extracting valuable insights from large datasets, and providing more accurate predictions. Machine learning (ML) techniques can be effectively employed for automatic detection of coastlines using various types of geospatial data, including satellite imagery, aerial photography, or LiDAR data (Seale *et al.*, 2022; Jaramillo *et al.*, 2022; Mao *et al.*, 2022). Both machine and deep learning approaches have been used for coastline detection (Seale *et al.*, 2022; Mao *et al.*, 2022). Deep learning was used for automated extraction of coastline morphology data from Sentinel-2 images, and four convolutional neural network (CNN) models, categorical cross-entropy loss, Sørensen–Dice loss and two novel loss functions, gave optimistic results for water/land separation (Seale *et al.*, 2022). A Random Forest model utilizing the first geomorphic Principal Component Analysis (PCA) component was employed for the global prediction of coastal geomorphic classification. Machine learning methods effectively discerned beaches, bedrock, and wetlands within various coastal systems on a global scale ranging from 56° S to 60° N (Jaramillo *et al.*, 2022). A flowchart illustrating the utilization of machine learning (ML)/deep learning (DL) techniques for analyzing coastal changes is depicted in Figure (6).

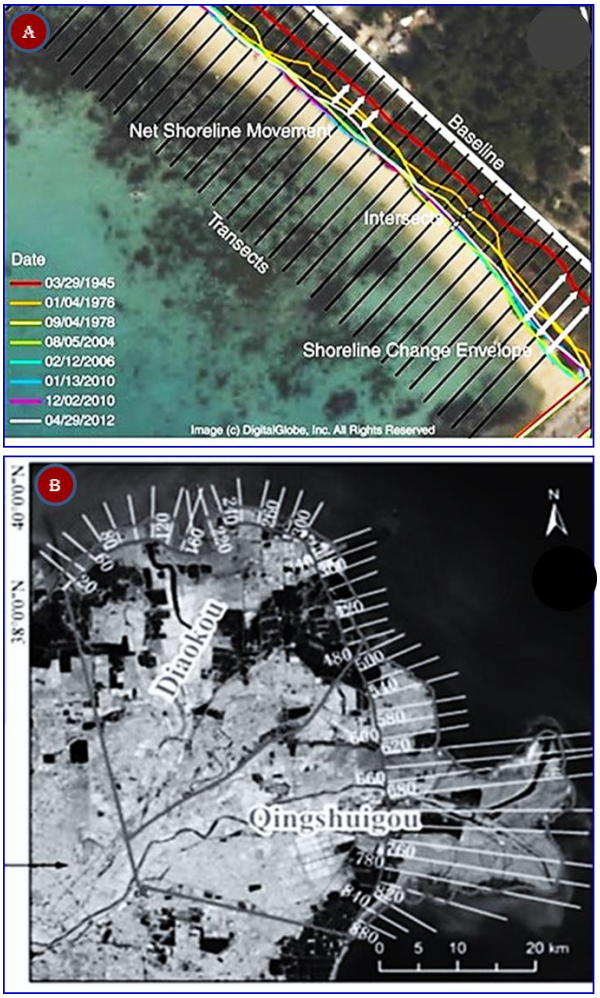

Figure (5). Examples of applied transforms of DSAS techniques. (a) French coast after (Ford, 2013), and (b) Yellow river delta after (Liu *et al.*, 2020b).

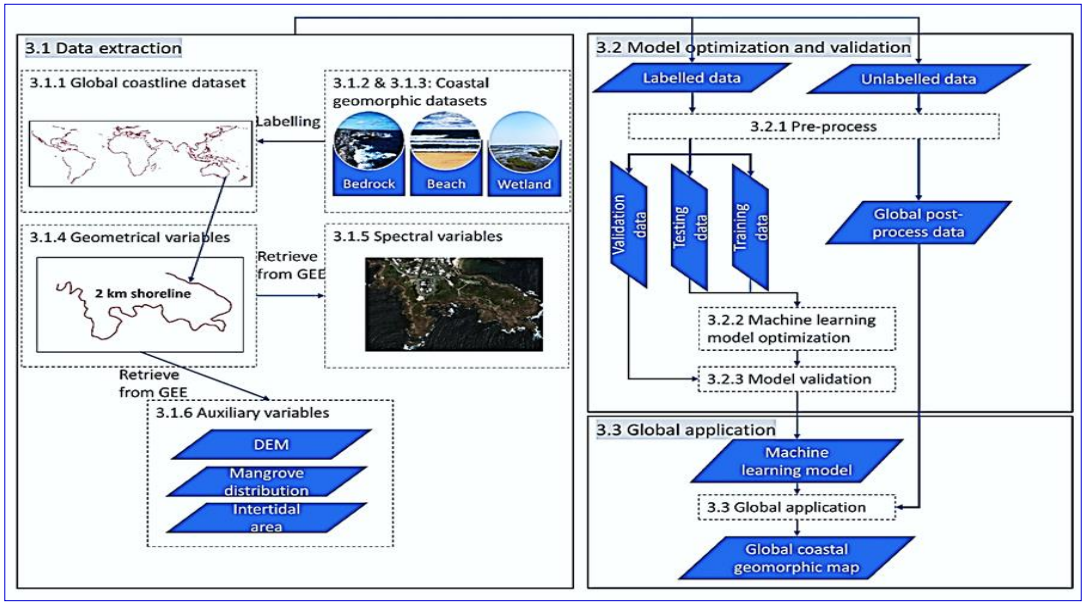

Figure (6): Flowchart of using machine learning/ deep learning Models for global coastal geomorphology, after (Mao *et al.*, 2022).

Spatial Analyses in Coastal Management

This study analyzed eighty-three publications on the topic of remote sensing and GIS technology of coastal monitoring published between 2012 and 2022. The statistical analysis of the global distribution of the literature shows three groups. The first group represents 47% of the studies performed in four countries: China, Spain China, Spain, South Korea and France.

The second group consisted of the USA, Australia, Brazil and Egypt, which comprised 28% of the published studies. The last group was composed of thirteen countries: Turkey, Benin, Canada, the Caribbean, Colombia, Ghana, Holland, India, Indo-nesia, Italy, the Marshall Islands, Poland, and Portugal, which comprised 25% of the studies. The following is a summary of studies published by continent, as shown in Figures (7) and (8).

Long-term Coastline Dynamics

Asian Coastline

The results indicated that Asian coasts were one of the highest global studies assessed in this study, and Landsat multi temporal images, Google Earth images, aerial photographs, and drone imagery were the essential datasets for coastal change assessment during the period from 1973 to 2020 along the Delta, Bays, Harbors, and Tidal Flats coasts.

In China, the coastal change in the East China Sea between 1985 and 2017 was assessed using Landsat imagery. The study detected changes in coastlines and tidal flats, and the results indicated that tidal flats decreased by 6%, while the land area increased by 18% (Cao *et al.*, 2020). This area has been subjected to infilling for fish farming and other agricultural activities. Spatiotemporal dynamic assessments of coastal tidal flats along China's coasts between 1986 and 2016 were studied using Landsat time series. The results indicated that due to intensive and ecological water diversion projects, tidal flats were converted into aquatic farms and saltpans. In addition, a large area of surface water (approximately 3.5 × 107 m3) was added to the Yellow River Delta in 2011 (Wang *et al.*, 2018).

Landsat imagery (30 m footprint) was used to assess the relationship between human activities and natural coastline changes in Xiangshan Harbor in China between 1974 and 2014. Erosion occurred for five periods (1974-82, 1982-90, 1990-98, 1998-2006, and 2006-2014), representing losses of 3.8 km, 4.6 km, 4.0 km, 0.5 km and 0.6 km/yr., respectively. The average rate of erosion was 2.7 km/yr. due to human activities (Li *et al.*, 2018). Coastline changes along Laizhou Bay in China from 1985 to 2017 showed an increase in coa astline length (from 460 km to 686 km), with a total increase of 226 km (Liu *et al*., 2020).

Multi temporal Landsat imagery was utilized to monitor human-induced changes on the Ningbo coastline in China between 2002 and 2018, and the results indicated that the length of the coastline increased from 176 km to 219 km (Li *et al.*, 2020).

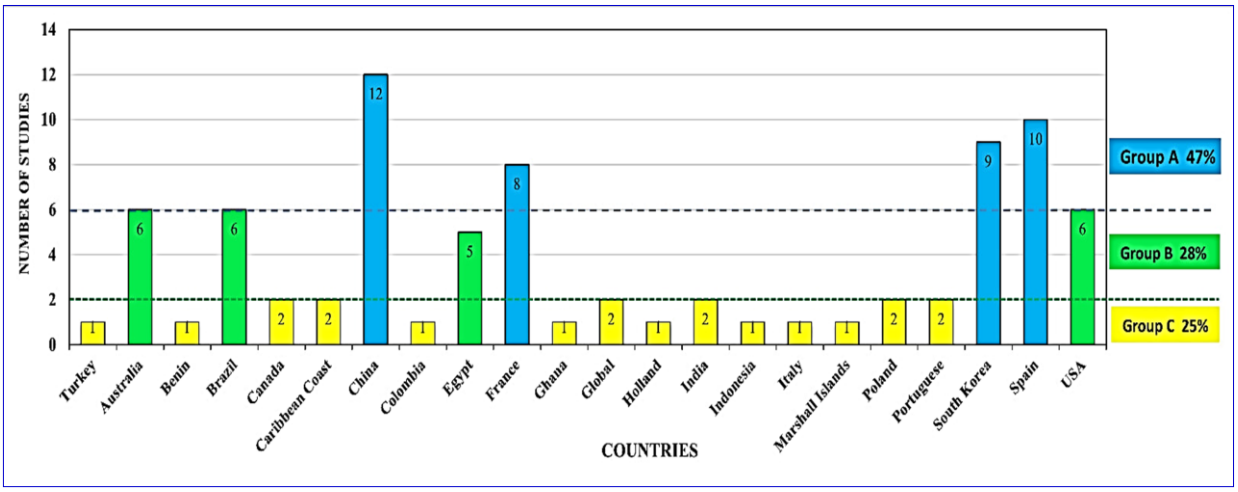

Figure (7): Contribution of global coasts in literature reviews

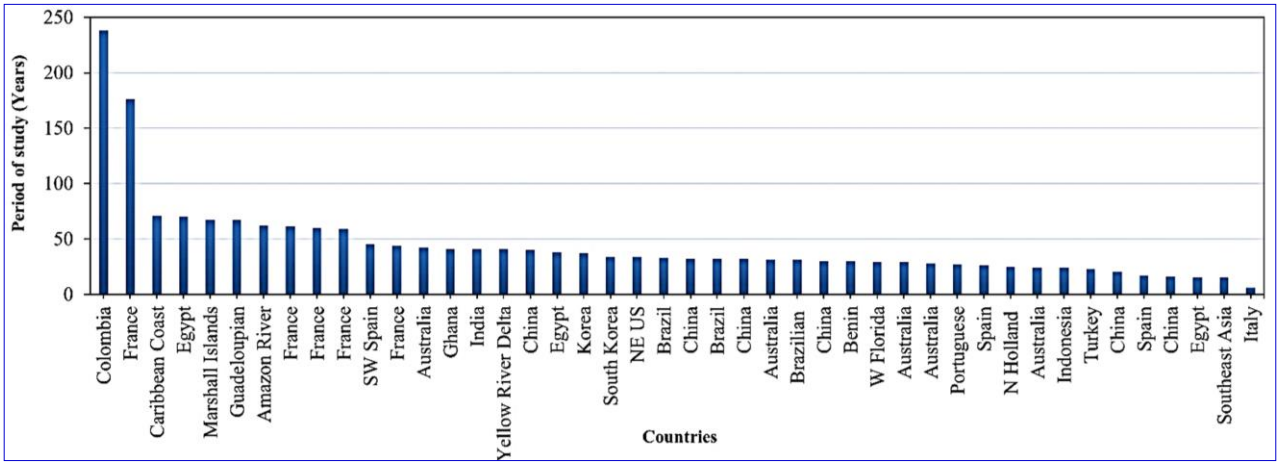

Figure (8): Distribution of Long-Term study periods across world countries.

Landsat imagery was used to extract and assess the coastline dynamics of mainland southeast Asia between 2000 and 2015 based on Google Earth images and the global distribution of mangrove data. The results showed that while the natural coastline length decreased from 15,440 km to 14,909 km, artificial coastlines increased from 3088 km to 3985 km. The major observed changes were in Myanmar, Vietnam, and Malaysia (Song *et al.*, 2020).

In Indonesia, analysis of coastal dynamics was carried out using a combination of Landsat and Google Earth imagery along the Cirebon coast between 1996 and 2020. Accretion averaged 5 m/yr., but 29% of the coastline eroded during the same time (Abdurrahman *et al.*, 2021) (Figure 9). The coastline change in South Korea was detected by comparing manned aerial photographs taken in 1986 with drone-based aerial photographs taken in 2020. The results indicated that coastlines accreted 100 m, and their elevation increased 4.9 m (Yun *et al*., 2021). Change analysis of the Krishna-Godavari delta region on the east coast of India from 1973 to 2014 using Landsat imagery. The results show that accretion occurred due to artificial spits and sand bars. It was observed that during the 40 years of analysis of the Godavari Delta River mouths, all were eroding. They included Nilarevu, which eroded 781 m; Gautami, which eroded 2.2 km; Vainateyam, which eroded 463 m; and Vasishta, which eroded 320 m. The Krishna delta accreted between 1973 and 1993 (Reshma and Murali, 2018).

Australian Coastline

Long-term coastal change studies along Australian coasts have utilized a combination of multi temporal Landsat imagery as well as aerial photographs for a period extended from 1987 to 2019. Spectral indices, a GIS-based digital shoreline analysis system and a deep learning approach were used for shoreline change analysis. A multi decadal study of mangrove vegetation change along the Australian mainland and the Tasmanian coastline was performed for the period 1987 to 2016 using Landsat imagery. The study found that there were many changes, mainly losses, in mangroves along the northern Australian coastline (Lymburner *et al.*, 2020).

Landsat imagery taken between 1988 and 2019 was extracted from the Landsat 5, 7, and 8 datasets and downloaded from Digital Earth Australia's data cube. Python programming, subpixels and the MNDWI were used to analyze the coastlines. The results indicated that 22% of Australia's sandy nonrocky coastline either eroded or accreted; the higher erosion rates were -3.5 m/yr. along the southern Van Diemen Gulf coast in the northwestern Australian coast, and -14.5 m/yr. along Point Stuart in the Northern Territory. The average accretion rate was +1.7 m/yr. along the mangrove coast of the southern Carpentaria Gulf with a maximum of 9.8 m/yr. (Bishop–Taylor *et al*., 2021) (Figure 10). The coastal dynamics of the Cape Jaffa Marina and canal estate in South Australia were studied using aerial photography taken between 1975 and 2005 using ML techniques. The results showed that accretion occurred updrift along the marina's entrance, and erosion occurred at the marina's walls and entrance (DaSilva *et al*., 2021).

European Coastline

Remote sensing plays a crucial role in monitoring and managing European coastlines, providing valuable information for environmental protection, resource management, and hazard assessment. European coastlines are diverse, facing challenges such as erosion, sea-level rise, habitat degradation, and human activeties. The coastline dynamics of northern France were assessed over a nearly 60-year period from 1946 to 2005 using aerial photographs, and the results showed that the Hardelot and Sainte Cécile coasts were eroding at 82% of the locations (Chaaban *et al.*, 2012). Changes in coastlines between 1950 and 2010 along France's west coast were assessed using aerial photography. The results indicated that 45 km of coast accreted, 78 km were stable and 46 km eroded. There was 2.8 km^2 of accreting surface and 1.1 km^2 of eroding surface (Robin *et al.*, 2019). 460 km of coastline along the southwestern France coast used maps published in 1840 and aerial photographs taken in 1945, 1973, 2000 and 2010) and satellite images taken in 2014 and 2016. The maximum mean erosion rate (14 m/yr.) was observed to the south of the Arvert Peninsula in southwestern France between 1999 and 2017 (Figure 11).

Long-term coastal accumulation in Brittany was studied. The researchers compared two sets of aerial photographs taken between 1949 and 2009. The results showed that 38% of the coasts were stable and 27% accreted (Stéphan *et al.*, 2019). Figure (12) shows the multi-temporal coastline change analysis along the SW French coast from 1950 to 2010. Analyses of coastline changes along the coasts of Spain were studied by (Pardo-Pascual *et al.*, 2012; Puig *et al*., 2014; Aps *et al.*, 2014). Landsat images taken between 1984 and 2010 were used to automatically extract the coastline and perform change analysis. The mean positional error of coastlines ranged from 3.5 to 2.8 m, with an average of 0.7 m, remaining stable over time. Changes in the coastline along SW Spain's coast were measured using aerial photographs taken between 1956 and 2010. The results indicate that the northern part of the Valdelagrana sand spit had an accretionary trend with stabilization in the past two decades.

In Turkey, coastline and land-use/cover changes in the basin of Terkos Lake were examined using Landsat satellite images taken in 1986, 2001 and 2009. The maximum shoreline change measured was 280 m over a period of 23 years (Bayram *et al.*, 2013). The Portuguese coasts were studied using Landsat images taken between 1984 and 2011. The resulting images showed a general trend of coastal erosion retreat of 3 m/yr. The maximum rate was 10 m/yr. (Cenci *et al.*, 2013). However, in Holland, coastline change between 1985 and 2010 using Landsat imagery was assessed. The results show accretion with an annual average ranging from 8 m to 9 m over 25 years (Do *et al.*, 2019).

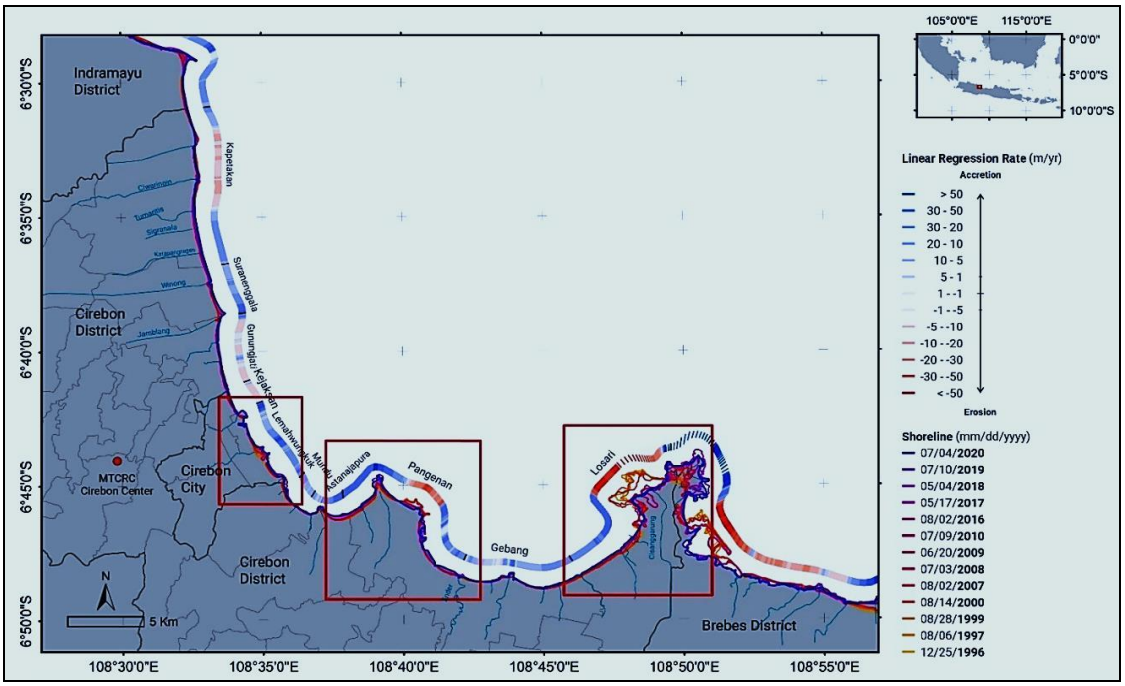

Figure (9): Coastline Change for the Cirebon Coast, after (Abdurrahman *et al.*, 2021).

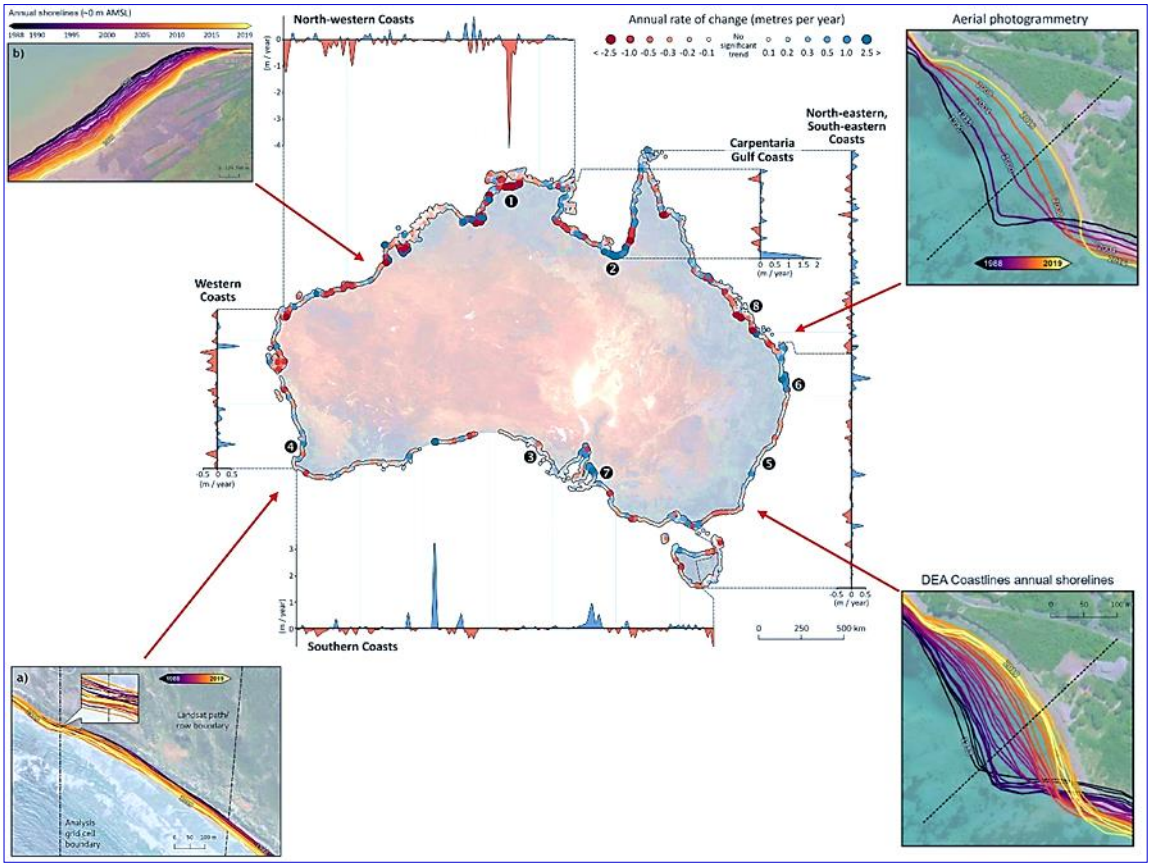

Figure (10): Time series Coastline Change in Australia between 1988 and 2019, modified after (Bishop–Taylor *et al.*, 2021), Subfigures show coastline advance and retreat techniques using machine leaning and other artificial intelligence methods.

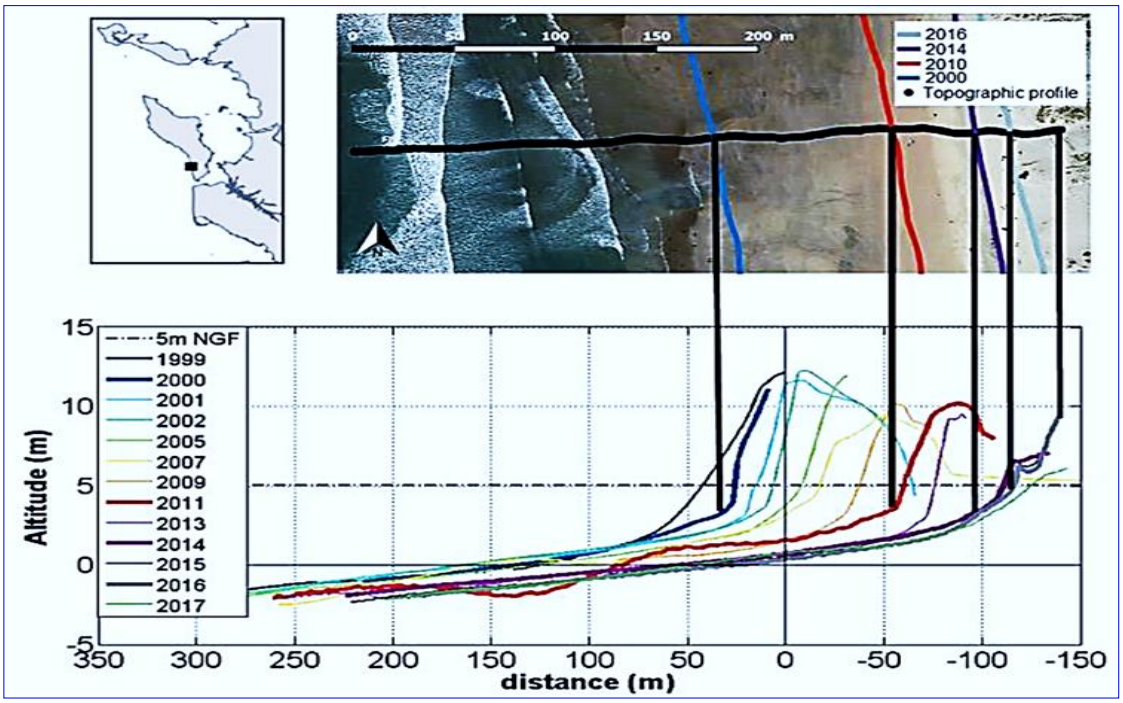

Figure (11): Coastline Change using spatial and vertical profile-technique for SW France between 1999 and 2017, after (Chaumillon *et al.*, 2019)

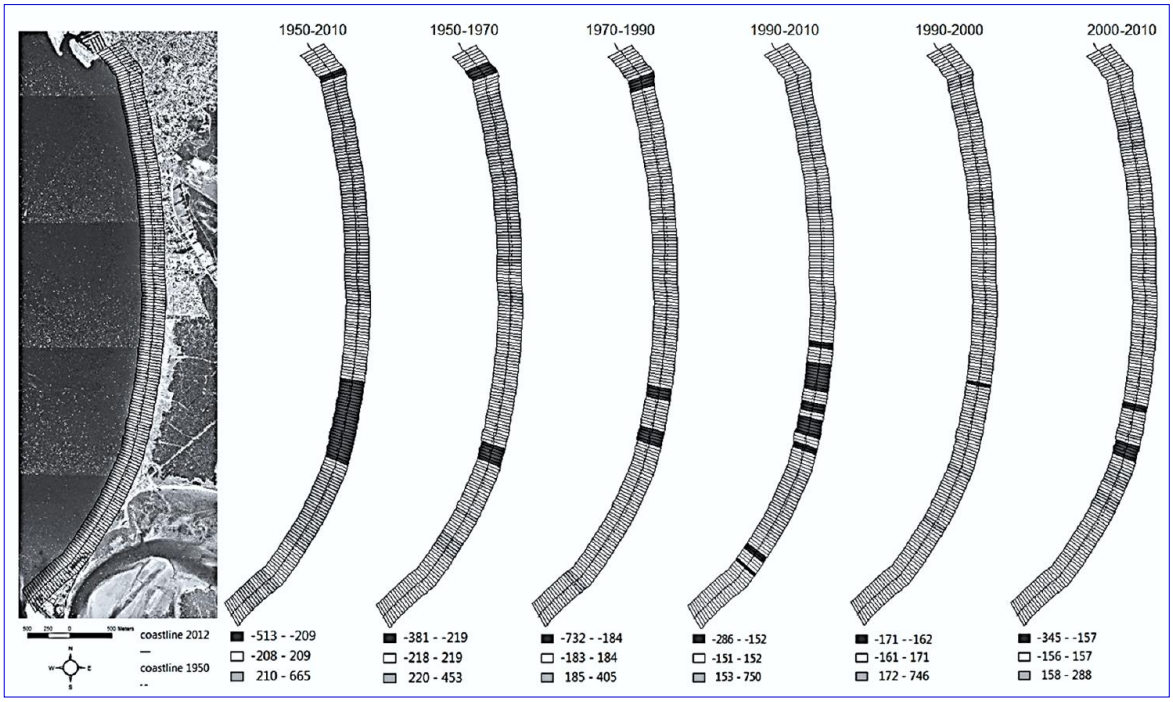

Figure (12): DSAS-based spatial computational technique for coastline change along the West Coast of France between 1950 and 2010 (Robin *et al.*, 2019)

The Americas Coastline

Geospatial technology provides a comprehensive and dynamic approach to coastline detection and analysis in the Americas. The integration of satellite imagery, LiDAR data, GIS, and other tools enables stakeholders to make informed decisions for sustainable coastal development, environmental conservation, and disaster resilience. Landsat time series taken between 1984 and 2013 were used to measure continuous coastal changes in western Florida, showing that muddy coasts in western Florida eroded at an average annual rate of 0.42±0.05 km²/year (Li and Gong, 2016).

Coastal tidal wetlands along the northeastern Atlantic coast of the United States were analyzed from 1986 to 2020 using Landsat imagery, and the results indicate that 12% changed, with vegetation decreasing by 2.6 km2 per year (Yang *et al.*, 2022). Changes in shoreline along the U.S. east coast salt marches indicated that 49% of transects were retreating and 51% were advancing between 1933 and 2013 in the Georgia Coastal Ecosystems (Burns *et al.*, 2021).

Coastal Changes in Brazil and Colombia: A Historical Analysis

The coastline of Brazil was mapped using Landsat imagery taken between 1984 and 2017 (Diniz *et al*., 2020). Brazil's coastal dynamics between 1988 and 2019 were determined by tracing the spring high tide level, showing that the coast lost 80 km² but gained approximately 83 km² (Teixeira *et al.*, 2021). Additionally, coastline changes between 1822 and 2018 along Colombia's northwest region were studied, using a map from 1822 and Google Earth imagery from 2018. The results indicate that erosion in the Cartagena de Indias region was high (González Rodríguez *et al*., 2021).

African Coastline

Studies of geomorphological changes along the Nile Delta coastline began using topographic maps in 1945. Landsat imagery has been used to map Egypt's Mediterranean and Red Sea coastlines since 1973. Much of the focus of the earliest studies was for the purpose of understanding the impacts of the Aswan High Dam, which was completed in 1970. There was concern that because the AHD had a trap efficiency of 99% and no sluice gates, all the sediment that formed the delta would be deposited behind the dam, and none would renourish the Mediterranean coastline. Therefore, erosion was expected at the two points where the Nile emptied into the Mediterranean Sea. Numerous studies using satellite remote sensing were used, especially after the construction of seawalls built along the Rosetta and Damietta promontories between 1984 and 2001 accretion (Darwish *et al.*, 2017).

Estimation of the impact of sea level rise in Ghana for the period 1974 to 2015 was performed using Landsat images and aerial orthophotos. Sea level rose 5.3 cm over 21 years. It accounts for 31% of the erosion rate of 2.0 m/yr. (Evadzi *et al.*, 2017). Benin coastal dynamics were studied using imagery taken between 1988 and 2018. SPOT and Sentinel-2 imagery were used, and the coastal features were extracted using the high-water line as an indicator. The coastline feature dynamics were analyzed using the Digital Shoreline Analysis System extension in ArcGIS. The results show accretion on 80% of the country's coastline. Between 2001 and 2012, 85% of the coastline was impacted by erosion, averaging 4.5 m/yr. From 1988 to 2018, accretion was observed along 68% of the coastline at an average rate of 0.9 meters per year. Conversely, erosion affected 31% of the coastline, occurring at an average rate of 0.7 meters per year. The majority of this erosion was concentrated near the mouth of the Bouche du Roy estuary (Balle *et al.*, 2021).

Short-Term Coastline Change Analysis

Table (2) summarizes the short-term coastline dynamics that have been researched in many locations across the world utilizing satellite remote and GIS techniques. The erosion/accretion pattern along the Damietta promontory shoreline in Egypt was established using synthetic aperture radar interferometric (InSAR) data collected by European remote-sensing satellites (ERS-1 and ERS-2) between 1993 and 2000. The findings indicated that four locations along the promontory shoreline experienced crucial erosion, with average rates of -9, -39, -17, and -11 m/yr. (El-Asmar *et al.*, 2014). To map the position of the shoreline and ascertain its movement, annual airborne LIDAR surveys were carried out along the Texas Gulf of Mexico shoreline between 2010 and 2012. The results indicate that during storm recovery, the shoreline advanced at 75% of the 11,783 monitoring sites and moved an average of 6.5 m seaward (Paine *et al.*, 2017).

August 15, 2012, observed the collection of the NE Pacific Ocean, Coastal Morphology, and Shore Zone Classification from airborne scanning LIDAR Terrain Models throughout the central coast of British Columbia, Canada. With an overall accuracy of 90%, LIDAR algorithms recognize the kind of substrate based on morphological features for five substrate classes: rock, rock and sediment, gravel, sand, and mud (Nijland *et al.*, 2017). In a macrotidal setting, the migration rates of two swash bars on a French ebb delta are investigated. The movement of the swash bar crests is calculated using a dataset of 12 LiDAR surveys conducted between 2011 and 2017. The results showed that bars moved 350–400 meters along the ebb tidal delta between 2011 and 2017 (Le Bas and Levoy Levoy, 2018).

Using shipborne mobile LiDAR systems, it is far more effective to monitor coastal changes along Anmok Beach, Korea, from January 2016 (winter season) to September 2016 (summer season) than using terrestrial LiDAR systems for measurements without shadow zones in foreshore areas. The summer coastline moved approximately 19 meters to the landward side from the winter coastline in the northern half of the survey area, and it changed slightly to the seaward side in the southern part. In comparison to the winter coastline, the summer coastline moved approximately

31 m landward and approximately 39 m seaward (Kim *et al.,* 2017). The muddy coastal zone in Sheyang city in Jiangsu Province, China, was imaged using many remote sensing techniques to determine coasts, with the assumption that shorelines are constant over short time periods (2014–2018). For artificial and muddy coastal locations, this approach could extract coastlines with high precision; however, it is not suitable for estuary areas (Wang *et al.,* 2020).

The Shatt Al-Arab Delta (northwestern Arabian/Persian Gulf) had a short-term geoinformatics assessment from 1971 to 2016. The findings show considerable alterations in the locations along the shoreline in addition to in the rates of silt buildup and erosion. Furthermore, the mapping of coastal dynamics has demonstrated notable shoreline migration, with variations between the left and right banks of the river mouth and a greater intrusion of salinity up the channel (Al-Aesawi *et al.,* 2020).

Factors Influencing Coastal Change

Natural Impacts of Coastline Dynamics

Marine climate of extreme events of changes in the shoreline are affected by natural forces such as sea level rise, hurricanes, cyclones, storm surges, hurricanes, and climate change. The implications of marine climate impacts on shoreline morph dynamics have been discussed in several studies included in this research. Table 3 provides a summary of research on the effects of anthropogenic and natural changes to the coast.

Waves and Currents

Large banks of mud, supplied by the Amazon River, move along the coast of the Amazon and Orinoco Guianas as a result of waves and currents; greater wave energy can cause extensive and quick erosion of the shoreline. Ten very-high resolution (0.4 - 1.5 m) aerial photographs that were chosen from a catalog covering 56 years, from 1955 to 2012, were used to examine multidecadal coastline alteration in the Guianas (Jolivet *et al.,* 2019).

Storm Surges

Using aerial photos, a correlation between storms and coastline changes was conducted along the Gulf of Cadiz (SW Spain). The findings showed that erosion rates are detected along both research sites, with varying contributions from storminess. In exposed places, erosion rates are higher due to storm activity (Puig *et al.,* 2014). Five terrestrial LiDAR measurements were conducted in Poland between November 2016 and April 2017 to assess the short-term cliff erosion linked to two significant storm surges and other minor storms in the town of Międzyzdroje. The first significant effect, according to the results, is a noticeable decrease in beach levels. a consequence of how frequently the storms occurred, the beach was unable to recuperate between the surges, which allowed the waves to directly hit the foot of the cliff (Terefenko *et al.,* 2018). The Copenhagen coast is subjected to impact assessments and mitigation of coastal storm surges through the use of GIS modeling techniques with LIDAR-based DTM. A combined raster representing the inundation level necessary to flood each individual terrain cell was created from a range of inundation scenarios for the capital of Copenhagen, ranging from 1.0 to 3.9 m. The scenarios were developed using an ArcGIS Pro workflow by Esri (Balstrøm and Kirby, 2022).

Cyclones, hurricanes and typhoons

October 2016 experienced the impact of an extratropical hurricane in southern Brazil, generating speculation about a possible connection between this occurrence and recent destructive occurrences. An estimated coastline retraction balance of 5.91 meters has been associated with the cyclone that occurred between October 26 and 27, 2016, according to a comparison of shoreline position data from the July 2016 image and the UAV (obtained in September and November 2016) (Albuquerque *et al.,* 2018). To assess the consequences of Hurricanes Allen (1980) and Ivan (2004) on Worthing Beach, Barbados, the DSAS employed four historical aerial photographs (1973, 1982, 1991, and 2004). The results showed that Hurricane Allen (1980) had an extremely quick accretion rate of 7.0 m/y. Following Hurricane Ivan's (2004) movement, over 110 meters of beachfront were removed while the hurricane continued to influence the island (Nagdee *et al.,* 2020).

Using airborne LIDAR databases, the results of Hurricane Michael, which devastated the USA on October 10, 2018, were assessed. The storm surge, which was approximately five meters high, wrecked the shoreline along the northwestern Florida coast. Hurricane Michael provides an outstanding opportunity to research how a powerful hurricane affects diverse coastal environments with different degrees of human development (Kelly and Gontz, 2020). Storm-Driven Morphodynamics of a Sandy Beach in Florida, The study examines the long-term morphological and morphological evolution of Casey Key in Sarasota County, Florida, as a consequence to significant storms and human activity using LIDAR data and historical Google Earth imagery. Although struck during the 2004 hurricane season, when it is estimated that 608,094 m3 of sand were lost and 50 m of retreat occurred in certain locations that threaten homes and beach development, Casey Key has generally shown resilience to erosion, especially an 8-km-long center portion (Jose and Carlin, 2022).

Sea-Level Rise Due to Climate Change

Coastline recession is caused by of sea level rise driven by climate change and has emerged as one of the greatest challenges threatening our world. The projected future beach destruction along Thailand's coasts relative to the 1986–2005 reference period is evaluated using the Bruun rule and the Coupled Model Comparison Project, Phase 5 (CMIP5) sea level rise scenarios for 2081-2100.

The national beach loss rates for RCP2.6, RCP4.5, RCP6.0, and RCP8.5 are estimated to increase to 45.8%, 55.0%, 56.9%, and 71.8% in the future, respectively. RCP2.6 and RCP8.5, for example, will lead to sandy beaches to disappear throughout 23 of the

51 zones (Ritphring *et al*., 2018). The susceptibility of Korea's coastal regions to disasters has been assessed in order to manage and increase the importance of these regions effectively. These are included in the Coastal Disaster Vulnerability Index (CDVI) along with resilience. The exposure indicators included typhoons, surges, waves, tides, SLR, and coastal erosion (Kang *et al*., 2018).

Coastal Vulnerability Index

The South Sinai coastline's vulnerability to climate change is calculated by the coastal vulnerability index (CVI), which takes into consideration the following shoreline characteristics: coastal slope, coastal geomorphology, fauna/flora, and socioeconomic components. To determine the essential characteristics of the coast in this study area, GIS and remote sensing analyses were utilized. The 635 km long coast is exposed to high and very high coastal susceptibility to climate change, according to the results, and global warming could make the region's biological suffering worse (Hereher, 2015). This study assesses the susceptibility of two regions of the Rio de Janeiro coastline (SE Brazil) to coastal erosion and flooding: the 20-kilometer Ma-cumba/Recreio-Barra beachfront and the 40-kilometer Marambaia barrier island (MBI), which is largely uninhabited and at risk due to sea level rise, wave climate, and shoreline mobility. Carvalho and Guerra (2020) determined that Marambaia Barrier Island exhibits a significant degree of vulnerability.

Anthropogenic Impacts of Coastline Dynamics

The coastline change rate can be influenced by human activities such as river dams, coastal constructions, and changes in land use and cover (Geriesh, *et al.,* 2015). Between 1945 and 2015, the Nile Delta coast of Egypt experi-enced geomorphological change. Landsat imagery and historical topographic maps were used to analyze changes in the rates of erosion and coastal accretion prior to and during the construction of the Aswan High Dam between 1964 and 1970. Along the Nile delta promontories and major cities between 1984 and 2001, the study additionally investigated the accretion and erosion of the coastline prior to and following the construction of coastal structures (sea walls, groins, jetties, and detached breakwaters) (Darwish *et al.,* 2017). Brazil's coastal vulnerability is increased by human pressure along Uruguay's coastline, which is manifested in the construction of coastal structures and a high population density, especially at the Macumba/Recreio-Barra beaches (Carvalho and Guerra, 2020). Using LIDAR data collected in 2011, the coastline position along detached breakwaters along the Portuguese West Coast was identified. The results indicated that in the event that no additional actions are taken in the Vagueira region, the entire coastal stretch will continue to erode, which, depending on the availability of sediment, may have severe repercussions in some places (Araújo *et al*., 2014).

Coastline extraction and mapping from Remote Sensing Data

The digital extraction of coastlines from multicourse satellite remote sensing images is crucial due to the variation in the spatial and spectral characteristics of imagery and its related sensors. The uncertainty and positional accuracy of the extracted coastlines from medium-resolution imagery, such as Landsat, Sentinel, and ASTER, are lower than those from high-resolution satellite imagery, such as IKONOS, QuickBird, GeoEye, and RapidEye. Moreover, the use of spectral indices, image segmentation techniques, and deep learning algorithms will give a higher accuracy result than manual delineation

DISSCUSION

Coastal dynamics have been studied using aerial photography since the 1930s (Ford, 2013; Jaramillo *et al.,* 2020). A great deal of aerial photography of many coasts in the world was taken during World War II. Unfortunately, if they are not digitized, many of the photographs and negatives deteriorate with time and are no longer useful for high accuracy-requiring tasks. When film-based photographs moved away from a nitrate base to a more chemically stable base, historical photographs lasted longer. Any long-term study of a coast should start with aerial photography (Chaaban *et al.,* 2012; Stéphan *et al.,* 2019).

The availability, repetitiveness and affordability of medium spatial resolution satellites such as Landsat, SPOT and Sentinel make their imagery products an attractive choice for studying coastline dynamics (Carvalho and Guerra 2020; Balle *et al.,* 2021). Landsat was launched in 1972, taking it the satellite with the longest record of continuous imagery. Landsat imagery was used in coastal studies on all the world's continents. Higher spatial resolution satellite imagery, such as Sentinel, QuickBird, IKONOS, and GeoEye imagery, has also been used for coastal change assessments around the globe (Song *et al.,* 2020; DaSilva *et al.,* 2021; Yun *et al.,* 2021; Dai *et al.,* 2019; Nijland *et al.,* 2019).

Drone-based aerial imagery was used in Brazil, South Korea and the USA (Albuquerque *et al.,* 2018; Jun *et al.,* 2018). Aerial, terrestrial, and mobile LiDAR surveys were used along the US, Australian and Polish coasts. Unfortunately, drones are illegal in many countries and restricted in others. In addition, some navigation technology available to drone users in the USA cannot be exported due to the International Treaty on Arms Regulations (ITAR) regulations (Luque *et al.,* 2012; Jun *et al.,* 2018).

Remote sensing has achieved a critical role in mapping and monitoring coastal dynamics. What started out as simply tracing the coastline from aerial photographs now features automatic extraction of the coastline using very high-resolution satellite imagery and even higher resolution drone-based imagery (Hossain *et al.,* 2021). While some of the imagery, such as Google Earth, Sentinel and Landsat, is free to the public, much of the very high-resolution imagery is relatively expensive for less developed countries. Many of these countries, such as Egypt and Bangladesh, are located in low-lying deltas and are thus subject to large

land losses due to sea level rise. It is critical that they have access to the highest possible resolution imagery so that they can plan for the future.

This study indicated that the global trends of coastal environment studies using remote sensing technology and GIS tools refer to an increase in utilizing geospatial artificial intelligence (GeoAI), including its advanced techniques of machine learning (ML) and deep learning (DL), which have been widely used for coastal dynamic analysis, assessment and future prediction in recent years beginning in 2018 (Seale *et al.*, 2022). The use of mobile ship-based terrestrial LiDAR, aerial and space LiDAR technologies, land video remote sensing monitoring systems, high-resolution optical satellite imagery, aerial photogrammetry, and radar remote sensing has dramatically increased for coastal dynamic mapping, modeling and marine hazard assessment.

Coastline dynamic assessment is essential for integrated coastal zone management as well as coastal planning for sustainable development. Advanced remote sensing imaging systems such as optical, radar, hyperspectral, airborne LiDAR, and drone-based UAV imagery have become essential for accurate coastal studies to support spatial decision systems. It is recommended to conduct a comprehensive coastal dynamic assessment using remote sensing, geographic information systems (GIS), and artificial intelligence (AI) technologies.

CONCLUSION

The examination of global trends in coastline dynamics monitoring has demonstrated that the integration of satellite remote sensing with GIS has markedly improved the precision and effectiveness of tracking coastline changes. Advances in satellite technology, including enhanced spatial and temporal resolution, have permitted more detailed and frequent observations, facilitating superior detection and analysis of coastal dynamics. Satellite remote sensing offers extensive data coverage, which is indispensable for investigating vast and remote coastal regions. This information is vital for comprehending long-term trends and patterns in coastline movement and for making well-informed decisions regarding coastal management. The methodologies reviewed are applicable across various disciplines, including environmental monitoring, urban planning, disaster management, and climate change studies. This interdisciplinary utility underscores the necessity for continued investment in satellite and GIS technologies. The reviewed studies indicate a strong correlation between climate change and coastline dynamics, with rising sea levels, increased frequency of extreme weather events, and human activities identified as key drivers of coastal erosion and accretion. Remote sensing and GIS are essential tools for quantifying these impacts and developing mitigation strategies. The ability to predict and visualize changes aids in formulating effective strategies for coastal protection, habitat conservation, and sustainable development. The review highlights the importance of global collaboration and data sharing to comprehensively address coastline dynamics. Future research should focus on developing more sophisticated algorithms, enhancing data fusion techniques, and ensuring the accessibility and interoperability of data across platforms. In conclusion, the rise of GeoAI for analyzing coastline dynamics can provide precise, timely, and comprehensive data, which is critical for addressing the challenges posed by natural and anthropogenic factors. Continued advancements and collaborative efforts are essential to fully harness these technologies for sustainable coastal management and resilience against climate change.

REFERENCES

ABD-ELHAMID, H.F., EL-KILANY, M.E., and JAVADI, A.A. 2015. A cost-effective method to protect the coastal regions from sea level rise a case study: Northern coasts of Egypt. J. Water Clim. Chang. 7, 114–127.

ABDURRAHMAN, U., DIASTOMO, H., AVRION-ESTI., SURYA, M.Y., BADRIANA, M.R., SUPRIJO, T., and PARK, H. 2021. Comprehensive analysis of coastal dynamics in Cirebon Coastal Area (CCA), Indonesia. In: Lee, J.L.; Suh, K.-S.; Lee, B.; Shin, S., and Lee, J. (eds.), Crisis and Integrated Management for Coastal and Marine Safety. J. Coast. Res. Special Issue No. 114, pp. 444–448. Coconut Creek (Florida), ISSN 0749-0208.

ABUALTAYEF, M., RABOU, M.A., and AFIFI, S. (2021). Change detection of Gaza coastal zone using GIS and remote sensing techniques. J Coast Conserv 25, 36. https://doi.org/10.1007/s11852-021-00825-4

ADNAN, F.A.F., HAMYLTON, S.M., and WOODROFFE, C.D. (2016). A Comparison of Shoreline Changes Estimated Using the Base of Beach and Edge of Vegetation Line at North Keeling Island. J. Coast. Res. Special Issue 75, 967–971.

AGHDAMI-NIA, M., SHAH-HOSSEINI, R., ROSTAMI, A., and HOMAYOUNI, S. (2022). Automatic Coastline Extraction through Enhanced Sea–Land Segmentation by Modifying Standard U-Net. Int. J. Appl. Earth Obs. Geoinf, 109, 102785.

AI, B., ZHANG, R., ZHANG, H., MA, C.L., and GU, F.G. (2019). Dynamic process and artificial mechanism of coastline change in the Pearl River Estuary. Reg. Stud. Mar. Sci. 30, 100715.

AL-AESAWI, Q., AL-NASRAWI, A., and JONES, B. (2020). Short-term geoinformatics evaluation in the Shatt Al-Arab delta (northwestern Arabian/Persian Gulf). J. Coast. Res. 36(3), 498–505. Coconut Creek (Florida), ISSN 0749-0208.

ALBUQUERQUE, M., ALVES, D., ESPINOZA, J., OLIVEIRA U., and SIMÕES R. (2018). Determining shoreline response to meteo-oceanographic events using remote sensing and unmanned aerial vehicle (UAV): case study in southern Brazil. In: Shim, J.-S.; Chun, I., and Lim, H.S. (eds.), Proceedings from the International Coastal Symposium (ICS), (Busan, Republic of Korea). J. Coast. Res.

Special Issue No. 85, pp. 766–770. Coconut Creek (Florida), ISSN 0749-0208.

ALY, M.H., GIARDINO, J.R., KLEIN, A.G., and ZEBKER, H.A. (2012). InSAR Study of Shoreline Change along the Damietta Promontory, Egypt," J. Coast. Res. 28(5), 1263-1269. https://doi.org/10.2112/JCOASTRES-D-11-00182.1

APS, R., TÕNISSON, H., ANFUSO, G., PERALES, J.A., ORVIKU, K., and SUURSAAR, Ü. (2014). Incorporating dynamics factor to the Environmental Sensitivity Index (ESI) shoreline classification—Estonian and Spanish example. J. Coast. Res. 70, 235–240.

ARAÚJO, M.C., DI BONA, S., and TRIGO-TEIXEIRA, A. 2014. Impact of detached breakwaters onshoreline evolution: a case study on the Portuguese west coast. In: Green, A.N. and Cooper, J.A.G. (eds.), Proceedings 13th International Coastal Symposium (Durban, South Africa). J. Coast. Res. Special Issue No. 70, pp. 041–046, ISSN 0749-0208.

ARNOUS, M.O., EL-RAYES, A.E., and EL-NADY, H. (2022). Flash flooding hazard assessment, modeling, and management in the coastal zone of Ras Ghareb City, Gulf of Suez, Egypt. J Coast Conserv 26, 77. https://doi.org/10.1007/s11852-022-00916-w

ARRIAGA, J., GABRIELA, M., ELENA, O., and PAULO, S. (2022). Shoreline Detection Accuracy from Video Monitoring Systems. Journal of Marine Science and Engineering 10, no. 1: 95. https://doi.org/10.3390/jmse10010095

BALLE, G.R., AHOUANSOU, D.M., SINTONDJI, L.C., and AGBOSSOU, E.K. (2021). Analyses of short- and long-term shoreline trends of the southwest Benin coast. J. Coast. Res. 37(2), 316–325. Coconut Creek (Florida), ISSN 0749-0208.

BALSTRØM, T., and KIRBY, J. (2022). A GIS-based screening workflow for coastal storm surge impact assessments and mitigation action consideration. J. Coast. Res. 38(4), 712–724. Coconut Creek (Florida), ISSN 0749-0208.

BAYRAM, B., SEKER, D.Z., ACAR, U., YUKSEL, Y., GUNER, A.H.A., and CETIN, I. (2013). An Integrated Approach to Temporal Monitoring of the Shoreline and Basin of Terkos Lake. J. Coast. Res. 29, 1427–1435.

BISHOP–TAYLOR, R., NANSON, R., SAGAR, S., and LYMBURNER, L. (2021). Mapping Australia's dynamic coastline at mean sea level using three decades of Landsat imagery. Remote Sens. Environ. 267, 112734.

BRUNO, M.F., MOLFETTA, M.G., MOSSA, M., NUTRICATO, R., MOREA, A., and CHIARADIA, M.T. (2016). Coastal observation through COSMO-skymed high-resolution SAR images. J. Coast. Res. 75, 795–799.

BURNS, C.J., ALEXANDER, C.R., and ALBER, M. (2021). Assessing Long-Term Trends in Lateral Salt-Marsh Shoreline Change along a U.S. East Coast Latitudinal Gradient, Journal of Coastal Research 37(2), 291-301. https://doi.org/10.21-12/JCOASTRES-D-19-00043.1.

CABEZAS-RABADÁN, C., PARDO-PASCUAL, J.E., PALOMAR-VÁZQUEZ, J., and FERNÁNDEZ-SARRÍA, A. (2019). Characterizing beach changes using high frequency Sentinel-2 derived shorelines on the Valencian coast (Spanish Mediterranean). Sci. Total Environ. 691, 216–231.

CAO, W., ZHOU, Y., LI, R., and LI, X. (2020). Mapping changes in coastlines and tidal flats in developing islands using the full time series of Landsat images. Remote Sens. Environ. 239, 111665.

Carvalho, B.C., and Guerra, J.V. (2020). Coastal vulnerability of Rio de Janeiro shoreline (SE Brazil) due to natural and social impacts. J. Coast. Res. 95 (SI), 759–763.

CENCI, L., DISPERATI, L., SOUSA, L., PHILLIPS, M., and ALVES, F. (2013). Geomatics for Integrated Coastal Zone Management: Multitemporal shoreline analysis and future regional perspective for the Portuguese Central Region. J. Coast. Res. 65, 1349–1354.

CHAABAN, F., DARWISHE, H., BATTIAU-QUENEY, Y., LOUCHE, B., MASSON, E., KHATTABI, J.E., and CARLIER, E. (2012). Using ArcGIS ® modelbuilder and aerial photographs to measure coastline retreat and advance: North of France. J. Coast. Res., 28, 1567–1579.

CHAUMILLON, E., CANGE, V., GAUDEFROY, J., MERCLE, T., BERTIN, X., and PIGNON, C. (2019). Controls onshoreline changes at pluri-annual to secular timescale in mixed-energy rocky and sedimentary estuarine systems. In B. Castelle, & E. Chaumillon (Eds.), Vol. 88. Coastal evolution under climate change along the tropical overseas and temperate metropolitan France (pp. 135–156). J. Coast. Res., Special Issue.

COLLIN, A., DUVAT, V., PILLET, V., SALVAT, B., and JAMES, D. (2018). Understanding Interactions between Shoreline Changes and Reef Outer Slope Morphometry on Takapoto Atoll (French Polynesia). J. Coast. Res. 85, 496–500.

CROSSLAND, C.J., BAIRD, D., DUCROTOY, J.-P., LINDEBOOM, H., BUDDEMEIER, R.W., DENNISON, W.C., MAXWELL, B.A., SMITH, S.V., and SWANEY, D.P. (2005). The Coastal Zone-A Domain of Global Interactions. In Coastal Fluxes in the Anthropocene: The Land-Ocean Interactions in the Coastal Zone Project of the International Geosphere-Biosphere Programme; Crossland, C.J., Kremer, H.H., Lindeboom, H.J., Marshall Crossland, J.I., Le Tissier, M.D.A., Eds.; Global Change-The IGBP Series; Springer: Berlin/Heidel-berg, Germany, pp. 1–37.

Cui, B., Jing, W., Huang, L., Li, Z., and Lu, Y. (2021). SANet: A Sea–Land Segmentation Network Via Adaptive Multiscale Feature Learning," in IEEE Journal of Selected Topics in Applied Earth Observations and Remote Sensing, vol. 14, pp. 116-126, doi: 10.1109/JSTARS.2020.3040176.

DAI, C., HOWAT, I.M., LAROUR, E., and HUSBY, E. (2019). Coastline extraction from repeat high-resolution satellite imagery. Remote Sens. Environ. 229, 260–270.

DARWISH, K., and SMITH, S. (2021). A Comparison of Landsat-8 OLI, Sentinel-2 MSI and PlanetScope Satellite Imagery for Assessing Coastline Change in El-Alamein, Egypt. Eng. Proc, 10, 23. https://doi.org/10.3390/ecsa-8-11258

DARWISH, K., and SMITH, S. (2023). Landsat-Based Assessment of Morphological Changes along the Sinai Mediterranean Coast between 1990 and 2020. Remote Sens. 15, 1392. https://doi.org/10.33-90/rs15051392.

DARWISH, K., SMITH, S.E., TORAB, M., MONSEF, H., and HUSSEIN, O. (2017). Geomorphological Changes along the Nile Delta Coastline between 1945 and 2015 Detected Using Satellite Remote Sensing and GIS. J. Coast. Res, 33, 786–794. https://doi.org/10.2112/JCOASTRES-D-16-00056.1.

DARWISH, K.S. (2023). Assessment of the Nile Delta's Coastline Dynamics: A Remote Sensing and GIS-Based Computational Approach. In: Hazard Modeling and Assessment of the Nile Delta Coast. Springer, Cham. https://doi.org/10.1007/978-3-031-44324-4_3

DASILVA, M., MIOT DA SILVA, G., HESP, P.A., BRUCE, D., KEANE, R., and MOORE, C. (2021). Assessing shoreline change using historical aerial and RapidEye satellite imagery (Cape Jaffa, South Australia). J. Coast. Res. 37(3), 468–483. Coconut Creek (Florida), ISSN 0749-0208.

DEWI, R.S., and BIJKER, W. (2020). Dynamics of shoreline changes in the coastal region of Sayung, Indonesia. Egypt J. Remote Sens. Space Sci. 23, 181–193.

DI, K., MA, R., WANG, J., and LI, R. (2003). Coastal mapping and change detection using high-resolution IKONOS satellite imagery. In Proceedings of the 2003 annual national conference on Digital government research, Boston, MA. vol.130, pp 1-4.

DINIZ, M.T., SILVA, D.S., SANTOS, J.R., SOUZA, R.M., and SILVA, J.P. (2020). Variation of the coastline between the years of 1984 and 2017 in the State of Sergipe, Northeast Region, Brazil. In: Malvárez, G. and Navas, F. (eds.), Global Coastal Issues of 2020. J. Coast. Res. Special Issue No. 95, pp. 458–462. Coconut Creek (Florida), ISSN 0749-0208.

DO, A.T., DE VRIES, S., and STIVE, M.J. (2019). The estimation and evaluation of shoreline locations, shoreline-change rates, and coastal volume changes derived from Landsat images. J. Coast. Res. 35, 56–71.

EL-ASMAR, H., EL-KAFRAWY, S., and TAHA, M. (2014). Monitoring Coastal Changes along Damietta Promontory and the Barrier Beach toward Port Said East of the Nile Delta. Egypt. J. Coast. Res. 30, 993–1005.

EVADZI, P.I., ZORITA, E., and HÜNICKE, B. (2017). Quantifying and predicting the contribution of sea-level rise to shoreline change in Ghana: Information for coastal adaptation strategies. J. Coast. Res, 33, 1283–1291.

FAN, Q., LIANG, L., LIANG, F., and SUN, X. (2020). Research progress on coastline change in China. In: Zheng, C.W.; Wang, Q.; Zhan, C., and Yang, S.B. (eds.), Air-Sea Interaction and Coastal Environments of the Maritime and Polar Silk Roads. J. Coast. Res. Special Issue No. 99, pp. 289–10. Coconut Creek (Florida), ISSN 0749-0208.

FORD, M. (2013). Shoreline changes interpreted from multitemporal aerial photographs and high resolution satellite images: Wotje Atoll, Marshall Islands. Remote Sens. Environ. 135, 130–140.

GASC, J., GACHE, C., BERTUCCI, F., MOUSSA, R.M., WAQALEVU, V., and LECCHINI, D. (2021). Effects of Coastline Modification on Coral Reef Fish Nurseries (Moorea, French Polynesia), Journal of Coastal Research 37(4), 842-851. https://doi.org/10.2112/JCOASTRES-D-20-00060.1

GERIESH, M., EL-RAYES, A., GOMAA, R., KAISER, M., and MOHAMED, M. (2015). Geoenvironmental impact assessment of El-Salam Canal on the surrounding soil and groundwater flow regime, Northwestern Sinai, Egypt. Catrina: The International Journal of Environmental Sciences, 12(1), 17-29.

GERRITY, B., PHILLIPS, M.R., and CHAMBERS, C. 2018. Applying a Coastal Vulnerability Index to San Mateo County: Implications for Shoreline Management In: Shim, J.-S.; Chun, I., and Lim, H.S. (eds.), Proceedings from the International Coastal Symposium (ICS), (Busan, Republic of Korea). J. Coast. Res. Special Issue No. 85, pp. 1406–1410. Coconut Creek (Florida), ISSN 0749-0208.

GERIESH, M., EL-RAYES, A., GOMAA, R., KAISER, M., and MOHAMED, M. (2015). Geoenvironmental impact assessment of El-Salam Canal on the surrounding soil and groundwater flow regime, Northwestern Sinai, Egypt. Catrina: The International Journal of Environmental Sciences, 12(1), 17-29.

GIRAUD-RENARD, E., DOLIQUE, F., COLLIN, A., JAMES, D., GAIRIN, E., COURTEILLE, M., BEAUFORT, O., RENÉ-TROUILLEFOU, M., DULORMNE, M., JEANSON, M., and LECCHINI, D. (2022). Long-term evolution of the Guadeloupean shoreline (1950–2017). J. Coast. Res. 38(5), 976–987. Coconut Creek (Florida), ISSN 0749-0208.

GONZÁLEZ RODRÍGUEZ, S.V., VALDECANTOS, V.N., DIEZ, J.J., DEL CAMPO, J.M., and ANTÓN, M.M. 2021. Comparing the effects of erosion and accretion along the coast of Cartagena De Indias, Colombia. J. Coast. Res. 37(6), 1204–1223. Coconut Creek (Florida), ISSN 0749-0208.

GUASTELLA, L.A., SMITH, A, M., and BREETZKE, T. (2014). Coastal management and mis-

management: comparing successes and failures at two lagoon outlets in KwaZulu-Natal, South Africa. In: Green, A.N. and Cooper, J.A.G. (eds.), Proceedings 13th International Coastal Symposium (Durban, South Africa), J. Coast. Res. Special Issue No. 70, pp. 513–520, ISSN 0749-0208.

HEREHER, M. (2015). Assessment of South Sinai Coastal Vulnerability to Climate Change. J. Coast. Res. 31(6), 1469-1477. https://doi.org/10.2112/JCOASTRES-D-14-00018.1

HOSSAIN, M.S., MUSLIM, A.M., POUR, A.B., MOHAMAD, M.N., ALAM, S.M.R., NADZRI, M.I., and KHALIL, I. (2021). Mapping different types of shorelines from coarse-resolution imagery: Fuzzy classification method can deliver greater accuracy. J. Coast. Res. 37(2), 433–441. Coconut Creek (Florida), ISSN 0749-0208.

HSIAO, Y.S., HWANG, C., CHENG, Y.S., CHEN, L.C., HSU, H.J., TSAI, J.H., LIU, C.L., WANG, C.C., LIU, Y.C., and KAO, Y.C. (2016). High-Resolution depth and coastline over major atolls of South China Sea from satellite altimetry and imagery. Remote Sens. Environ. 176, 69–83. https://doi.org/10.2112/JCOASTRES-D-12-00247.1

IBRAHIM, M. S. (2021). Flash flood hazard prediction of Shalatin City, Red Sea Coast, Egypt utilizing HEC-RAS model. Catrina: The International Journal of Environmental Sciences, 23(1), 93-103.

JARAMILLO, C., SÁNCHEZ-GARCÍA, E., JARU, M.S., GONZÁLEZ, M., and PALOMAR-VASQUEZ, J.M. (2020). Subpixel satellite-derived shorelines as valuable data for equilibrium shore-line evolution models. J. Coast. Res. 36(6), 1215–1228.

JOLIVET, M., GARDEL, A., and ANTHONY, E. J. (2019). Multidecadal changes on the mud-dominated coast of western French Guiana: implications for mesoscale shoreline mobility, river-mouth deflection, and sediment sorting. J. Coast. Res. 82.

JOSE, F., and CARLIN, F. (2022). Storm-driven morphodynamics of a sandy beach in Florida. J. Coast. Res. 38(5), 896–907. Coconut Creek (Florida), ISSN 0749-0208.

JUN, K., JUN, B.-H., LEE, H., KIM, S., and TAK, W. 2018. The study of utilization and precision based on the comparison and analysis of drone-based coastal hazard data and its application in the ocean environment. In: Shim, J.-S.; Chun, I., and Lim, H.S. (eds.), Proceedings from the International Coastal Symposium (ICS), (Busan, Republic of Korea). J. Coast. Res. Special Issue No. 85, pp. 811–815. Coconut Creek (Florida), ISSN 0749-0208.

KAISER, M.F. 2014. Disturbance of hydrodynamic regime in the Mediterranean coastal zone of Egypt. J. Coast. Res. 298, 1260–1267.

KANG, T., OH, H., LEE, E., and JEONG, K. 2018. Disaster Vulnerability Assessment in Coastal Areas of Korea. In: Shim, J.-S.; Chun, I., and Lim, H.S. (eds.), Proceedings from the International Coastal Symposium (ICS) 2018 (Busan, Republic of Korea). J. Coast. Res. Special Issue No. 85, pp. 886–890. Coconut Creek (Florida), ISSN 0749-0208.

KELLY, J.T., and GONTZ, A.M. 2020. Rapid assessment of shoreline changes induced by Tropical Cyclone Oma using CubeSat imagery in southeast Queensland, Australia. J. Coast. Res. 36(1), 72–87. Coconut Creek (Florida), ISSN 0749-0208.

KIM, C., KIM, H., PARK, C., KIM, W., LEE, M., CHOI, S., and DO, J. 2018. Coastline change measurement using shipborne mobile LiDAR in Anmok Beach, Gangneung, Korea. In: Shim, J.-S.; Chun, I., and Lim, H.S. (eds.), Proceedings from the International Coastal Symposium (ICS), (Busan, Republic of Korea). J. Coast. Res. Special Issue No. 85, pp. 601–605. Coconut Creek (Florida), ISSN 0749-0208.

KIM, H., LEE, S.B., and MIN, K.S. 2017. Shoreline change analysis using airborne LiDAR bathymetry for coastal monitoring. In: Lee, J.L.; Griffiths, T.; Lotan, A.; Suh, K.-S., and Lee, J. (eds.), the 2nd International Water Safety Symposium. J. Coast. Res. Special Issue No. 79, pp. 269–273. Coconut Creek (Florida), ISSN 0749-0208.

KIM, Y. J., KIM, T. W., YOON, J.-S., HUR, D. S, and KIM, M. K. 2021. Shoreline change prediction for integrated coastal erosion management. In: Lee, J.L.; Suh, K.-S.; Lee, B.; Shin, S., and Lee, J. (eds.), Crisis and Integrated Management for Coastal and Marine Safety. J. Coast. Res. Special Issue No. 114, pp. 121–125. Coconut Creek (Florida), ISSN 0749-0208.

LE BAS, X., and LEVOY, F. (2018). Bar migrations on a macrotidal ebb delta over a period of six years using LiDAR survey. In: Shim, J.-S.; Chun, I., and Lim, H.S. (eds.), Proceedings from the International Coastal Symposium (ICS) 2018 (Busan, Republic of Korea). J. Coast. Res. Special Issue No. 85, pp. 146–150. Coconut Creek (Florida), ISSN 0749-0208.

LEE, H.Y., JEONG, Y.H., KIM, D.H., KIM, D.S., CHO, W.H., and HONG, S.J. 2020. Effects of Large-Scale Coastal Construction on Storm Surge Height in Shallow Coastal Zones of the Yellow Sea, South Korea, Journal of Coastal Research 95(sp1), 252-256. https://doi.org/10.2112/SI95-049.1

LI, J., PU, R., YUAN, Q., LIU, Y., FENG, B., GUO, Q., JIANG, Y., and YE, M. 2018. Spatiotemporal Change Patterns of Coastlines in Xiangshan Harbor (Zhejiang, China) During the Past 40 Years. J. Coast. Res. 34, 1418–1428.

LI, W.Y., and GONG, P. 2016. Continuous monitoring of coastline dynamics in western Florida with a 30-year time series of Landsat imagery. Remote Sens. Environ. 179, 196–209.

LI, X., and DAMEN, M. 2010. Coastline change detection with satellite remote sensing for environmental management of the Pearl River Estuary, China. J. Mar. Syst. 82, S54–S61.

LI, Y., WEI, B., SUO, A., ZHANG, Z., XU, Y., and LIANG, Y. 2020. Spatial and temporal coupling relationships of coastline exploitation and

environmental carrying safety in Ningbo, China. J. Coast. Res. 36(6), 1292–1301. Coconut Creek (Florida), ISSN 0749-0208.

LIST, J.H., SALLENGER, A.H., HANSEN, M.E., and JAFFE, B.E. 1997. Accelerated relative sea-level rise and rapid coastal erosion: Testing a causal relationship for the Louisiana barrier islands. Mar. Geol. 140, 347–365.

LIU, C., CHANG, J., CHEN, M., and ZHANG, T. 2020a. Dynamic monitoring and its influencing factors analysis of coastline in the Laizhou Bay since 1985. In: Hu, C. and Cai, M. (eds.), Geo-informatics and Oceanography. J. Coast. Res. Special Issue No. 105, pp. 18–22. Coconut Creek (Florida), ISSN 0749-0208.

LIU, H., and JEZEK, K. 2014. Automated extraction of coastline imagery by integrating Canny edgy detection and locally adaptive thresholding methods. Int. J. Remote Sensing. 25 (5), 937–958.

LIU, Y., LI, X., and HOU, X. 2020b. Spatiotemporal changes to the river channel and shoreline of the Yellow River Delta during a 40-year period (1976–2017). J. Coast. Res. 36(1), 128–138. Coconut Creek (Florida), ISSN 0749-0208.

LUIJENDIJK, A., HAGENAARS, G., RANASINGHE, R., BAART, F., DONCHYTS, G., and AARNINKHOF, S. (2018). The State of the World's Beaches. Sci. Rep. 8, 1–11.

LYMBURNER, L., BUNTING, P., LUCAS, R., SCARTH, P., ALAM, I., PHILLIPS, C., TICEHURST, C., and HELD, A. 2020. Mapping the multi-decadal mangrove dynamics of the Australian coastline. Remote Sens. Environ. Volume 238, 111185.

MAO, Y., HARRIS, D. L., XIE, Z., and PHINN, S. 2022. Global coastal geomorphology–integrating earth observation and geospatial data. Remote Sens. Environ. 278, 113082.

MELET, A., TEATINI, P., LE COZANNET, G., JAMET, C., CONVERSI, A., BENVENISTE, J., and ALMAR, R. 2020. Earth Observations for Monitoring Marine Coastal Hazards and Their Drivers. Surv. Geophys. 41, 1489–1534.

MENTASCHI, L., VOUSDOUKAS, M., PEKEL, J.-F., VOUKOUVALAS, E., and FEYEN, L. 2018. Global long-term observations of coastal erosion and accretion. Sci. Rep. 8, 12876. https://doi.org/10.1038/s41598-018-30904-w.

MOORE, L., MCNAMARA, D., MURRAY, A., and BRENNER, O. 2013. Observed changes in hurricane-driven waves explain the dynamics of modern cuspate shorelines. Geophys. Res. Lett. 40, 5867–5871.

MOUSTAFA, A.A., ABDELFATH, A., and ARNOUS, M.O. 2023. Monitoring temporal changes in coastal mangroves to understand the impacts of climate change: Red Sea, Egypt. J Coast Conserv 27, 37 . https://doi.org/10.1007/s11852-023-00970-y

MURALI, R.M., RESHMA, K.N., KUMAR, S.S., BALAJI, S.A., RAJU, D.M.K., and RAMAKRISHNAN, R. 2020. Spatiotemporal coastal morphological changes of Godavari delta region in the east coast of India. In: Malvárez, G. and Navas, F. (eds.), Global Coastal Issues. Journal of Coastal Research, Special Issue No. 95, pp. 626–631. Coconut Creek (Florida), ISSN 0749-0208.

NAGDEE, M.R., NURSE, L., INNISS, L., CHADWICK, A., and JOHNSON, T. 2020. Historical shoreline mapping: Application of the Digital Shoreline Analysis System to the evolution of Worthing Beach, Barbados, following Hurricanes Allen (1980) and Ivan (2004). J. Coast. Res. 36(2), 313–318. Coconut Creek (Florida), ISSN 0749-0208.

NIJLAND, W., RESHITNYK, L., and RUBIDGE, E. 2019. Satellite remote sensing of canopy-forming kelp on a complex coastline: A novel procedure using the Landsat image archive. Remote Sens. Environ. 220, 41–50.

NIJLAND, W., RESHITNYK, L.Y., STARZOMSKI, B.M., REYNOLDS, J.D., DARIMONT, C.T., and NELSON, T.A. 2017. Deriving Rich Coastal Morphology and Shore Zone Classification from LiDAR Terrain Models. J. Coast. Res. 33(4), 949-958. https://doi.org/10.2112/JCOASTRES-D-16-00109.1

NOAA. 2022. What Is Remote Sensing? National Ocean Service Website. Available online: https://oceanservice.noaa.gov/facts/remotesensing.html (accessed on 14 August 2022).

PAINE, J.G., CAUDLE, T.L., and ANDREWS, J.R. (2017). Shoreline and Sand Storage Dynamics from Annual Airborne LIDAR Surveys, Texas Gulf Coast," J. Coast. Res. 33(3), 487-506. https://doi.org/10.2112/JCOASTRES-D-15-002-41.1

PANIAGUA-ARROYAVE, J.F., CORREA, I.D., ANFUSO, G., and ADAMS, P.N. (2018). Soft-cliff retreat in a tropical coast: the Minuto de Dios sector, Caribbean Coast of Colombia. J. Coast Res. 81, 40–49.

PARAVOLIDAKIS, V., RAGIA, L., MOIROGI-ORGOU, K., and ZERVAKIS, M.E. 2018. Automatic Coastline Extraction Using Edge Detection and Optimization Procedures. Geosciences, 8, 407. https://doi.org/10.3390/g-eosciences8110407.

PARDO-PASCUAL, J.E., ALMONACID-CABALLER, J., RUIZ, L.A., and PALOMAR-VAZQUEZ, J. 2012. Automatic extraction of shorelines from Landsat TM and ETM+ multitemporal images with subpixel precision. Remote Sens. Environ. 123, 1–11.

PENG, F., DENG, X., and CHENG, X. 2021. Quantifying the precision of retracked Jason-2 sea level data in the 0-5 km Australian coastal zone. Remote Sens. Environ. 263, 112539. https://doi.org/10.1016/j.rse.2021.112539.

PILKEY, O.H.; and HUME, T. 2001. The shoreline erosion problem: lessons from the past. Water Atmos. 9 (2), 22-23.

POITEVIN, C., WOPPELMANN, G., RAUCOULES, D., LE COZANNET, G., MARCOS, M., and

TESTUT, L. 2019. Vertical land motion and relative sea level changes along the coastline of Brest (France) from combined space-borne geodetic methods. Remote Sens. Environ. 222, 275–285.

PUIG, M., DEL RIO, L., PLOMARITIS, T.A., and BENAVENTE, J. 2014. Influence of storms on coastal retreat in SW Spain. J. Coast. Res. 70, 193–198.

RESHMA, K.N., and MURALI, R.M. 2018. Current status and decadal growth analysis of Krishna-Godavari delta regions using remote sensing. J Coast Res, 85: 1416–1420.

RITPHRING, S., SOMPHONG, C., UDO, K., and KAZAMA, S. 2018. Projections of Future Beach Loss due to Sea Level Rise for Sandy Beaches along Thailand's Coastlines. J. Coast. Res. 85, 541–545.

ROBIN, M., JUIGNER, M., LUQUET, F., and AUDÈRE, M. 2019. Assessing surface changes between shorelines from 1950 to 2011: The case of a 169-km sandy coast, Pays de la Loire (W France). J. Coast. Res. 88, 122–134.

SAGAR, S., ROBERTS, D., BALA, B., and LYMBURNER, L. 2017. Extracting the intertidal extent and topography of the Australian coastline from a 28-year time series of Landsat observations. Remote Sens. Environ. 195, 153–169.

SEALE, C., REDFERN, T., CHATFIELD, P., LUO, C., and DEMPSEY, K. 2022. Coastline detection in satellite imagery: A deep learning approach on new benchmark data. Remote Sens. Environ. 278, 113044.

SONG, Y., LI, D., and HOU, X. 2020. Characteristics of mainland coastline changes in Southeast Asia during the 21st century. J. Coast. Res. 36, 261–275.

STÉPHAN, P., EMMANUEL, B., SERGE, S., BERNARD, F., RONAN, A., FRANCE, F., VÉRONIQUE, C., NICOLAS, D., JÉRÔME, A., LAURENCE, D., MARION, J., and CHRIST-OPHE, D. 2019. Long, medium, and short-term shoreline dynamics of the Brittany Coast (Western France). J Coast Res. 88 (sp1): 89-109. https://doi.org/10.2-112/SI88-008.1.

SUO, A., and ZHANG, M. (2015). Sea areas reclamation and coastline change monitoring by remote sensing in coastal zone of Liaoning in China. J. Coast. Res, 73, 725–729.

TAK, W.J., JUN, K.W., KIN, S.D., and LEE, H.J. 2020. Using drone and LiDAR to assess coastal erosion and shoreline change due to the construction of coastal structures. In: Malvárez, G. and Navas, F. (eds.), Global Coastal Issues of 2020. J. Coast. Res. Special Issue No. 95, pp. 674-678. Coconut Creek (Florida).

TEIXEIRA, S.G., BANDEIRA, I.C.N., and DANTAS, M.E. 2021. Shoreline variation and identification of local erosion geoindicators on the Brazilian Amazon coast. J. Coast. Res. 37(6), 1088–1098. Coconut Creek (Florida), ISSN 0749-0208.

TEREFENKO, P., GIZA, A., PAPROTNY, D., KUBICKI, A., and WINOWSKI, M. 2018. Cliff Retreat Induced by Series of Storms at Międzyzdroje (Poland). In: Shim, J.-S.; Chun, I., and Lim, H.S. (eds.), Proceedings from the International Coastal Symposium (ICS) 2018 (Busan, Republic of Korea). J. Coast. Res. Special Issue No. 85, pp. 181–185. Coconut Creek (Florida).

THAKARE, L.M., and SHITOLE, T.A. 2021. Vulnerability assessment of the Ratnagiri coast (Maharashtra, west coast of India). J. Coast. Res. 37(2), 421–432. Coconut Creek (Florida), ISSN 0749-0208.

U.S. 2022a. Climate Resilience Toolkit. "Coastal Erosion https://toolkit.climate.gov/topics/coastal-flood-risk/coastal-erosion (accessed in September 4, 2022).

U.S. 2022b. Army Corps of Engineers. "Economic Implications of Shoreline Change https://www.iw-r.usace.army.mil/missions/coasts/national-shore-line-management/nsms-economic-implications-of-shoreline-change. (Accessed in August 14, 2022).

WAGHMARE, S., HANAMGOND, P., MITRA, D., KOTI, B., and SHINDE, P. (2020). Application of remote sensing and GIS techniques to study sediment movement along Harwada Beach, Uttar Kannada, west coast of India. J. Coast. Res. 36(6), 1121–1129. Coconut Creek (Florida), ISSN 0749-0208.

WANG, C., YANG, J., LI, J., and CHU, J. 2020. Deriving natural coastlines using multiple satellite remote sensing images. In: Jung, H.-S.; Lee, S.; Ryu, J.-H., and Cui, T. (eds.), Advances in Geospatial Research of Coastal Environments. J. Coast. Res. Special Issue No. 102, pp. 296-302. Coconut Creek (Florida).

WANG, P., ADAM, J.D., CHENG, J., and VALLÉE, M. 2020. Morphological and sedimentological impacts of Hurricane Michael along the northwest Florida coast. J. Coast. Res. 36(5), 932–950. Coconut Creek (Florida).

WANG, X., XIAO, X., ZOU, Z., CHEN, B., MA, J., DONG, J., DOUGHTY, R.B., ZHONG, Q., QIN, Y., and DAI, S. (2018). Tracking annual changes of coastal tidal flats in China during 1986–2016 through analyses of Landsat images with Google Earth Engine. Remote Sens. Environ.110987.

WILLIAMS, D., and KRAUS, N. 1999. Shoreline Change by Waves, Wind, and Tidal Current, Corpus Christi Bay, Texas. In Proceedings of the 4th International Symposium on Coastal Engineering and Science of Coastal Sediment Processes, Hauppauge, NY, USA, 21–23 June 1999; pp. 2219–2234.

WOZENCRAFT, J., DUNKIN, L., REIF, M., and EISEMANN, E. 2018. A spatial index approach to coastal monitoring: A Florida case study. In: Almar, R.; Almeida, L.P.; Trung Viet, N., and Sall, M. (eds.), Tropical Coastal and Estuarine Dynamics. J. Coast. Res. Special Issue No. 81, pp. 67–75. Coconut Creek (Florida).

WU, Q., MIAO, S., HUANG, H., GUO, M., ZHANG, L., YANG, L., and ZHOU, C. 2022. Quantitative Analysis on Coastline Changes of Yangtze River

Delta Based on High Spatial Resolution Remote Sensing Images. Remote Sens. 14, 310. https://doi.org/10.3390/rs14020310.

WU, T., and HOU, X. 2016. Review of research on coastline changes. Acta Ecol. Sin. 36, 1170–1182.

WU, T., HOU, X.Y., and XU, X.L. 2014. Spatiotemporal characteristics of the mainland coastline utilization degree over the last 70 years in China. Ocean. Coast. Manag. 98, 150-157.

XU, N. 2018. Detecting Coastline Change with All Available Landsat Data over 1986–2015: A Case Study for the State of Texas, USA. Atmosphere.9, 107. https://doi.org/10.3390/atmos9030107.

XU, N., and GONG, P. 2018. Significant coastline changes in China during 1991-2015 tracked by Landsat data. Sci. Bull. 63, 883–886.

YANG, X., ZHU, Z., QIU, S., KROEGER, K.D., ZHU, Z., and COVINGTON, S. 2022. Detection and characterization of coastal tidal wetland change in the northeastern US using Landsat time series. Remote Sens. Environ. 276, 113047.

YOUN, S., and ZARILLO, G. 2022. Morphological analysis of barrier islands in the Nakdong River Estuary, South Korea. J. Coast. Res. 38(3), 475–490. Coconut Creek (Florida), ISSN 0749-0208.

YOUNIS, A., ISMAIL, I., MOHAMEDEIN, L., and AHMED, S. 2014. Spatial variation and environmental risk assessment of heavy metal in the surficial sediments along the Egyptian Red Sea coast. Catrina: The International Journal of Environmental Sciences, 10(1), 19-26.

YUE, B., LIU, S., YAN. Z., LIAO, J., and GAO, M. 2021. Geomorphological Difference and Genesis of Typical Sandy Coasts in the Northern and Southern Shandong Peninsula," Journal of Coastal Research 37(2), 380-388. https://doi.org/10.2112/JCOASTRES-D-19-00178.1

YUN, K., LEE, C.K., HE, G., and PARK, B.W. 2021. Monitoring of shoreline change at Chollipo Beach in South Korea. In: Lee, J.L.; Suh, K.-S.; Lee, B.; Shin, S., and Lee, J. (eds.), Crisis and Integrated Management for Coastal and Marine Safety. J. Coast. Res. Special Issue No. 114, pp. 469-473. Coconut Creek (Florida), ISSN 0749-0208.

ZHANG, Y.Z., CHEN, R.S., and WANG, Y. 2020. Tendency of land reclamation in coastal areas of Shanghai from 1998 to 2015. Land Use Policy. 91, 104370.

ZHAO, X., WANG, X., ZHAO, J., and ZHOU, F. 2021. An improved water-land discriminator using laser waveform amplitudes and point cloud elevations of airborne LIDAR. J. Coast. Res. 37(6), 1158–1172. Coconut Creek (Florida), ISSN 0749-0208.

ZHOU, X.Y., ZHENG, J.H., DOONG, D.J., and DEMIRBILEK, Z. 2013. Sea level rise along the East Asia and Chinese coasts and its role on themorphodynamic response of the Yangtze River Estuary. Ocean Eng. 71, 40–50.

رَصد ديناميكيات خط الساحل باستخدام الاستشعار من بعد بالأقمار الصناعية ونظم المعلومات الجغرافية: مراجعة تحليلية للاتجاهات العالمية

كمال سروجي درويش
قسم الجغرافيا ،كلية الآداب،جامعة المنيا، مصر

الملخص العربـــــي

تساهم تكنولوجيا الاستشعار من بعد ونظم المعلومات الجغرافية في وضع حلول للعديد من المشكلات الطبيعية على سطح الأرض، وتعد ظاهرة التغير ات الجيومورفولوجية في خط الساحل الناتجة عن تأثير العديد من العوامل الطبيعية والبشرية أحد هذه الظاهرات المهمة. وتفيد دراسة خطوط السواحل في تحديد نطاقات أخطار التعرية الساحلية وتقدير معدلات تراجع الشواطئ وعلاقتها بالتغيرات المناخية وارتفاع منسوب سطح البحر بالإضافة إلى الأنشطة البشرية. تهدف هذه الدراسة الى تحليل الاتجاه العام والتحديدات في استخدام تقنيات الاستشعار من بعد عبر الأقمار الصناعية ونظم المعلومات الجغرافية في دراسات التغيرات الساحلية على المستوى العالمي بالاعتماد على تحليل ودراسة الدراسات المنشورة في الدوريات العلمية العالمية المفهرسة خلال الفترة من 2012 وحتى 2022. ويتضح من النتائج أن هناك تزايد كبير في الاعتماد على مرئيات الأقمار الصناعية المختلفة المصدر (لاندسات – سبوت – سينتينال – كويك بيرد – إيكونوس - جيوآي) في الاستخلاص الآلي لخطوط الشواطئ وتحليلها ونمذجتها في نظم المعلومات الجغرافية، كما تم الاعتماد مؤخرا على تقنيات المسح الجوي بالليدار واستخدام المركبات غير المأهولة وكاميرات الرصد الأرضي في المرقبة عالية الدقة للتغيرات الساحلية. كما بدأ التطور المذهل في علوم نظم المعلومات الجغرافية بعد دمج لوغاريتمات الذكاء الاصطناعي والتعلم العميق في برمجيات نظم المعلومات الجغرافية.